

Review

# Coal-Hosted Al-Ga-Li-REE Deposits in China: A Review

Yanbo Zhang, Xiangyang Liu and Wei Zhao \*

Shenhua Geological Exploration Co., Ltd., Changping, Beijing 102209, China; 10018120@chnenergy.com.cn (Y.Z.); 11685078@chnenergy.com.cn (X.L.)

\* Correspondence: 11685189@chnenergy.com.cn

**Abstract:** Investigation of the critical metal elements in coal and coal-bearing strata has become one of the hottest research topics in coal geology and coal industry. Coal-hosted Ga-Al-Li-REE deposits have been discovered in the Jungar and Daqingshan Coalfields of Inner Mongolia, China. Gallium, Al, and Li in the Jungar coals have been successfully extracted and utilized. This paper reviews the discovery history of coal-hosted Ga-Al-Li-REE deposits, including contents, modes of occurrence, and enrichment origin of critical metals in each coal mine, including Heidaigou, Harewusu, and Guanbanwusu Mines in the Jungar Coalfield and the Adaohai Coal Mine in the Daqingshan Coalfield, as well as the recently reported Lao Sangou Mine. Gallium and Al in the coals investigated mainly occur in kaolinite, boehmite, diaspore, and gorceixite; REEs are mainly hosted by gorceixite and kaolinite; and Li is mainly hosted by chlorite. Gallium, Al, and REEs are mainly derived from the sediment-source region, i.e., weathered bauxite in the Benxi Formation. In addition, REE enrichment is also attributed to the intra-seam parting leaching by groundwater. Lithium enrichment in the coals is of hydrothermal fluid input. The content of  $\text{Al}_2\text{O}_3$  and Ga in coal combustions (e.g., fly ash) is higher than 50% and  $\sim 100 \mu\text{g/g}$ , respectively; concentrations of Li in these coals also reach the cut-off grade for industrial recovery (for example, Li concentration in the Haerwusu coals is  $\sim 116 \mu\text{g/g}$ ). Investigations of the content, distribution, and mineralization of critical elements in coal not only provide important references for the potential discovery of similar deposits but also offer significant coal geochemical and coal mineralogical evidence for revealing the geological genesis of coal seams, coal seam correlation, the formation and post-depositional modification of coal basins, regional geological evolution, and geological events. Meanwhile, such investigation also has an important practical significance for the economic circular development of the coal industry, environmental protection during coal utilization, and the security of critical metal resources.



Academic Editors: Thomas Gentzis and Shifeng Dai

Received: 19 November 2024

Revised: 26 December 2024

Accepted: 26 December 2024

Published: 14 January 2025

**Citation:** Zhang, Y.; Liu, X.; Zhao, W. Coal-Hosted Al-Ga-Li-REE Deposits in China: A Review. *Minerals* **2025**, *15*, 74. <https://doi.org/10.3390/min15010074>

**Copyright:** © 2025 by the authors. Licensee MDPI, Basel, Switzerland. This article is an open access article distributed under the terms and conditions of the Creative Commons Attribution (CC BY) license (<https://creativecommons.org/licenses/by/4.0/>).

**Keywords:** critical elements; coal; Al-Ga-Li-REE deposit; Chinese coal

## 1. Introduction

Coal is one of the most complicated geological materials [1] and consists of various minerals and organic components with different chemical structures [2–7]. Coal uses have caused serious issues related to environmental pollution and human health [8–12]. However, coal remains a cornerstone of global energy production, currently largely supplying worldwide electricity [13,14]. Beyond power generation, coal is integral to numerous industries, including metallurgy, cement production, and chemical manufacturing [1]. Additionally, it serves as a critical heat source for sectors such as wallboard, aluminum, and cement production. Lesser known is coal's potential as a source of critical metals [15–17]. Many coals contain economically significant concentrations of such metals essential for

technological advancement, such as Li, Ga, U, Ge, V, rare earth elements (REEs), Y, Sc, Nb, Zr, Re, Au, Ag, platinum group elements (PGEs), W and Se, and base metals like Al and Mg [16,18–21]. These metals are indispensable for driving innovations in technology and energy efficiency [13,22,23], and therefore have attracted many researchers to reveal the abundance, modes of occurrence, distribution, and mineralization process of these critical metals in coal and coal ash [18,24–30]. It is commonly considered that coal is now one of the important sources for critical elements [31–36].

On the other hand, the dwindling supplies and escalating prices of these critical metals in traditional ore deposits [37,38], coupled with the concentrated control of production by a limited number of countries, e.g., China, has spurred a global quest for alternative sources [22,39]. Notably, China dominates the global production of rare earth elements (85%) and germanium (73%) [40,41]. Coal and its combustion byproducts offer a promising avenue for extracting these critical elements [34,41]. Some coal deposits and associated materials exhibit element concentrations comparable to, or even surpassing, those found in conventional ores [21]. The terms “coal-hosted rare-metal deposit” proposed by Dai and Finkelman [13] and “metalliferous coal” proposed by Seredin and Finkelman [21] have emerged to characterize coals rich in economically recoverable critical elements.

While extracting Al, Ga, Ge, U, V, and Se from coal/coal ash has been established for years [13,15,22,38,42–48], the recovery of Li, REY, Sc, Nb, and Zr represents a new frontier in coal utilization [29,31,49–52]. Some pilot plants for co-recovering rare earth elements and other critical materials have been successfully established in the USA. This emerging field has the potential to redefine coal’s role in the global economy [38].

## 2. Overview of Coal-Hosted Al-Ga-Li-REE Deposits

The Jungar Coalfield in Inner Mongolia, northern China, was identified as a novel critical metal deposit by researchers from China University of Mining and Technology (Beijing) (CUMTB) in 2006 [53,54]. This discovery is extremely important, as stated by Seredin [19]: *“significant steps forward in production of valuable metals from coal and for development of both traditional and alternative energy options. Thus, this operation is a good example that coal deposits, with insight from coal science, can be transformed into clean energy sources”*. The findings by these researchers (i.e., discovery of the ore deposit; the abundance, spatial distribution, and modes of occurrence of critical elements; the mechanism of mineralization of Al, Ga, Li, and REEs) [53–55] have laid a solid foundation for recovering Al, Ga, and Li from the coal combustion byproducts derived from coal power plants. This is also a typical case of turning coal, a traditional fossil fuel, into a green energy, on the basis of these important findings. Between 2011 and 2017, the deposit underwent seven successful trial runs for alumina production, meeting both quality and quantity targets. A 4000 t/y industrial pilot plant for extracting alumina and gallium from fly ash was successfully constructed by Shenhua Zhunneng Group in August 2011. In 2013, the first batch of metallic gallium was produced from the pilot plant. By 2021, a fourth-generation circulating fluidized bed combustion technology had been developed, utilizing nano-hydrocarbons as fuel for the high-efficiency extraction of aluminosilicate powder. A circular economy industrial chain has been formed, encompassing coal, electricity, fly ash, green electrolytic aluminum, and high-end aluminum products metallic gallium and lithium. The alumina produced exceeds the national standard for first-grade metallurgical-grade alumina, the metallic gallium surpasses the 4N purity standard, and the lithium carbonate meets battery-grade standards. Therefore, a comprehensive review of this deposit not only helps readers to have a full picture of the discovery history of the ore deposit, the origin of the ore formation, and the successful extraction of the critical metals, but also is useful for further discovering similar potential coal-hosted ore deposits in other areas.

Germanium from coal has been industrially recovered for more than half a century [14,19,40]. The recovery of rare earth elements is still on pilot-scale level, and a number of studies have shown promising extraction technologies [26,31,49,56–61] not only from coal ashes but also for non-coal rocks in coal-sedimentary sequences [33,62]. Although some studies have investigated the modes of occurrence and enrichment origin of Li in coal [25,32,33,42,57,63–67], the recovery technologies are still being investigated [52]. Uranium in coal has been industrially utilized [19,38]; however, it seems that U in coal has not attracted much attention in the last several decades, although some studies have shown significant enrichment of U in coal [22,34,45,68–74]. Although Sc enrichment has been found in some Russian coals [24], coals with highly enriched Sc have not been found in China [27,29,34,75–77] in spite of the varying geological conditions [6,78–80].

### 3. Geological Setting of the Jungar and Daqingshan Coalfields

The coal-hosted Al-Ga-Li-REE deposits in China were mainly discovered in the Jungar and Daqingshan Coalfields (Figure 1), which are close to each other. The two coalfields have similar sedimentary sequences, but the Jungar is situated on the margin of the Ordos Basin and the Daqingshan Coalfield is located within the Yinshan Orogenic Belt.

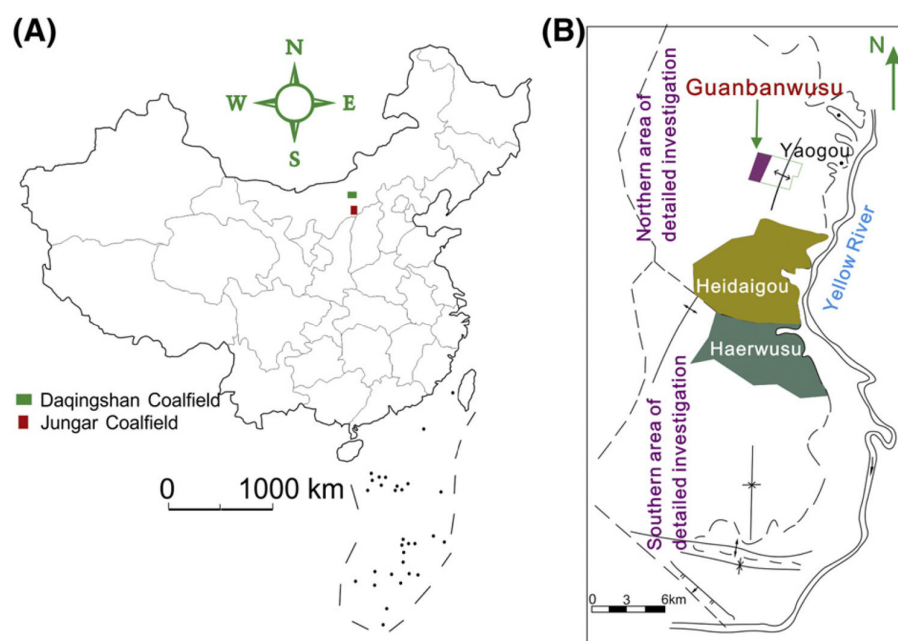


**Figure 1.** Location of the Jungar and Daqingshan Coalfields (A) and distribution of the Guanbanwusu, Heidaigou, and Haerwusu Mines in the Jungar Coalfield (B) [49].

#### 3.1. Jungar Coalfield

The Ordos Basin, one of the most famous depositional basins in China, contains abundant resources, including coal, oil, gas, uranium, and other non-metal resources [25,29,36], and is situated in the west of the Northern China Platform. The Jungar Coalfield lies on the Ordos Basin's northeastern margin. Measuring 65 km north–south and 26 km east–west, the coalfield covers an area of 1700 km<sup>2</sup>. As one of the Ordos Basin's most prolific coalfields, its reserves are estimated at 26.8 gigatons.

The sediments in Jungar Coalfield are characterized by a diverse range of sedimentary environments [81]. A gradual transition from limestone-dominated to predominantly clastic sediments is evident as limestone deposits thin out within the coalfield from south to north. Coal-bearing strata in the region comprise the Pennsylvanian Benxi and Taiyuan formations, as well as the Lower Permian Shanxi Formation, collectively reaching thicknesses between 110 and 160 m [53–55].

The Benxi Formation, with a thickness ranging from 15 to 35 m, unconformably overlies the Middle Ordovician Majiagou Formation. The overlying Taiyuan Formation, varying in thickness from 35 to 70 m, is composed primarily of quartzose sandstone, mudstone, siltstone, and coal seams intercalated with darker mudstone, siltstone, limestone, and thin quartzose sandstone layers. Lithological variations within the Taiyuan Formation are pronounced across the coalfield. In the southern regions, the formation is predominantly composed of terrigenous, coal-bearing clastic rocks, primarily sandstone, and contains five unminable coal seams (Nos. 1 to 5).

The upper portion of the Taiyuan Formation is composed of mudstone, sandy mudstone, and the No. 6 coal. The No. 6 coal, which has an average thickness of 30 m, is located at the top of the Taiyuan Formation. It is the major minable coal bed, accounting for approximately 80% of the total coal reserve in the Jungar Coalfield. The No. 6 coal is overlain by dark gray mudstone, sandy mudstone, or siltstone and underlain by mudstone. Superimposed on the coal-bearing sequences are the non-coal-bearing Upper and Lower Shihezi Formations, the Shiqianfeng Formation, and the Liujiagou Formation.

### 3.2. Daqingshan Coalfield

The Daqingshan Coalfield is located to the north of the Jungar Coalfield. Encompassing an area between 40°35' and 40°44' north latitude and 110°07' and 110°31' east longitude in Inner Mongolia, northern China, the Daqingshan Coalfield has 16 coal mines distributed across the coalfield [82–84]. Among these, the Adaohai Mine is situated in the southeastern part of the coalfield. The coal-bearing strata within the Daqingshan Coalfield, which includes the Pennsylvanian Shuanmazhuang and the Early Permian Zahuaigou formations [85–89], were deposited in a continental setting.

The Daqingshan Coalfield's primary coal seam, identified as CP2 coal, is situated in the upper portion of the Shuanmazhuang Formation, varying in thickness from 4.7 to 42.8 m, with an average of 22.3 m. The zoned distribution of coal rank of the CP2 coal within the coalfield is directly attributed to igneous intrusions that occurred during the Yanshan Movement [90]. In the eastern part of the coalfield, igneous rocks have intruded into the coal-bearing strata, resulting in a coal rank gradient that increases from northwest to southeast, transitioning from high volatile bituminous to medium volatile bituminous and ultimately to low volatile bituminous. The CP2 coal contains 3 to 42 parting layers ranging from 0.02 to 3.4 m in thickness. Due to epigenetic tectonic movements, the CP2 coal has been heavily brecciated and exhibits a dip of approximately 83 degrees. The overlying roof, primarily consisting of mudstone and sandy mudstone, has a fluctuating thickness. In certain areas, the CP2 coal directly contacts the overlying sandstone. The floor of the CP2 coal also demonstrates significant variations in thickness and lithology, ranging from 0.2 to 2.0 m and composed of sandy sandstones, medium coarse sandstones, and fine sandstones.

The lower part of the Shuanmazhuang Formation comprises conglomerate, granule conglomerate, sandy mudstone, siltstone, and thin coal seams. Overlying the Shuanmazhuang Formation, the Permian strata consist of the Zahuaigou and Shiyewan formations. The upper portion of the Zahuaigou Formation is composed of mudstones and sandstones, while the lower portion features white quartz-pebble conglomerate with locally intercalated 0.1–0.2 m mudstone beds. The Zahuaigou Formation lacks minable coal beds. The Shiyewan Formation is primarily composed of thick sandstone layers interbedded with mudstone. The Cambrian–Ordovician strata underlying the coal-bearing sequences are dominated by limestone, with intercalated silty mudstone in the lower part.

#### 4. Discovery of the Jungar Coal-Hosted Ore Deposit of Critical Metals

Coal and metal industries have traditionally operated independently. Yet, notable exceptions exist, as evidenced by two significant cases [21] that yielded mutual benefits and economic progress. A pioneering example involves the extraction of U from coals. In the United States and the former Soviet Union, high-U coals played a crucial role in post-WWII nuclear development [19]. Subsequently, the discovery of more substantial U reserves in other types of ore deposits rendered coal-based U extraction less economically viable. Another notable example is the extraction of Ge from coal [19,38], which commenced in the late 1950s and remains a significant industrial practice. Coal currently supplies over half of the global demand for Ge. In a brief commentary by Seredin [19], the author discussed the groundbreaking discovery made by Chinese coal geologists during 2005–2015, i.e., the findings of the coal-hosted Ga-Al-Li-REE deposits in Inner Mongolia, China.

Research initiated by CUMTB scientists in the early 2000s within the Heidaigou surface mine, Jungar Coalfield, Inner Mongolia, unveiled an extraordinary discovery of highly enriched critical metals in the No. 6 coal seam [19,53,54,91], the deposit's primary minable coal, with an average thickness of 30 m, exhibiting anomalous concentrations of  $\text{Al}_2\text{O}_3$  (>50%, ash basis) and gallium (up to 100  $\mu\text{g/g}$ , ash basis); the latter is a metal typically associated with Al [53]. Intriguingly, the coal's silica-to-alumina ratio (Si/Al) was exceptionally low compared to that of global coals, measuring as low as 0.34 [53,54], which was caused by highly enriched mineral boehmite, a rare mineral in coal composed of 84.9% alumina [3,4,72]. Boehmite, alongside kaolinite, served as the primary hosts of aluminum and gallium in these coals [53,54].

Samples of pristine fly ash were collected from the economizer of the Jungar power plant with a special sampling device, because the flue gas along with fly ash was disposed through wet ash concentration units [92]. Concentrations of critical elements in combustion byproducts (e.g., fly ash) confirmed these super-large aluminum and gallium deposits, not only covering the Heidaigou Mine in the Jungar Coalfield but also covering the Haerwusu and Guanbanwusu Mines [55,56] in this coalfield.

The recognition of fly ash as a potential source for recovering these metals marked a significant breakthrough [19]. Comprising approximately 90% of combustion waste, fly ash offered a substantial resource for recovery of these critical metals [22]. Analysis determined average aluminum and gallium concentrations in fly ash to be 51% and 92  $\mu\text{g/g}$  [92], respectively, mirroring those found in conventional bauxite deposits [19]. Additionally, the concentrations of REY in the fly ash derived from this coal seam were also high and a potential source for REY recovery [93,94]. This exceptional metal enrichment was due to neighboring bauxite deposits, which served as the erosional rocks for the peat during the Late Paleozoic, with aluminum and gallium subsequently accumulating in the peat deposit.

Confirmed reserves totaled 150 million tons of alumina and 49,000 tons of gallium in the Heidaigou Mine [53,54]. Aluminum and gallium are primarily concentrated in mullite and glass phases in the fly ash. Laboratory-scale extraction of alumina, silica gel, and gallium from fly ash proved successful [19]. Based on these findings, a pilot plant with an annual capacity of 800,000 tons of alumina and approximately 150 tons of gallium was established in early 2011.

Of significant note is the discovery of similar deposits in the Daqingshan Coalfield of Inner Mongolia, further confirming the importance of these coal-hosted Ga-Al deposits [55,82–84,95,96].

#### 5. Abundance and Modes of Occurrence of Critical Elements in Coals

The coal seams labeled as No. 6 and No. CP2 in the Jungar and Daqingshan Coalfields, respectively, were highly enriched in Al, Ga, Li, and REEs and were widely distributed in

the two coalfields. Although the two coal seams are labeled as different identities, they are the same coal seam [97]. The coals with highly evaluated Al, Ga, Li, and REEs in the Jungar coals are mainly distributed in the Heidaigou, Haerwusu, and Guanbanwusu Coal Mines. Recently, a new highly mineralized Al, Ga, Li, and REE coal seam was discovered in the Laosangou Coal Mine [98], which is located close to the Heidaigou Mine in the Jungar Coalfield. The coals with highly evaluated Al, Ga, Li, and REEs in the Daqingshan Coalfield are mainly distributed in the Adaohai, Datanhao, and Hailiushu coals.

There have been no cut-off standards for Al, Ga, Li, and REEs that are globally accepted for critical metals in coal, although some researchers have proposed some suggested cut-off grades for selected metals in coal. Considering the high concentrations of  $\text{Al}_2\text{O}_3$ , Ga, Li, and REEs in the Jungar and Daqingshan coals, establishing appropriate cut-off grades for these critical elements in coal combustion byproducts is essential. In 1980s, a Chinese standard recommendation of 30–50  $\mu\text{g/g}$  for Ga in coal (whole coal basis) was proposed CONMR (1987). However, other factors, as pointed out by Dai et al. [55] and Dai and Finkelman [13], including resources, thickness of coal seam, ash yields of raw coals, other associated critical elements, the possibility of beneficiation, market demand and supply, recovery technology, and environmental effects, must also be evaluated. Based on studies on  $\text{Al}_2\text{O}_3$  and Ga recovery technology, the chemistry and mineralogy of coal combustion products (e.g., fly ash and bottom ash), the thickness of coal seams, mineralogical and elemental associations, and pilot and industrial plants' experience in recovery of these metals from the Jungar coals [55], it is suggested that CCB with Ga concentrations exceeding 50  $\mu\text{g/g}$ , a ratio of  $\text{SiO}_2/\text{Al}_2\text{O}_3$  less than 1 (or  $\text{Al}_2\text{O}_3$  greater than 40% in CCB), and a coal thickness of the coal seam of at least 5 m (allowing for selective mining) could be suitable for  $\text{Al}_2\text{O}_3$  and Ga recovery from CCB [13,55].

The factors mentioned above should also be considered for rare earth elements (REY) and lithium. Experimental data on REY extraction from coal combustion byproducts (CCB) suggests a cut-off grade of 1000  $\mu\text{g/g}$  REO (oxides of rare earth elements plus Y) in ash for profitable recovery from low-rank coals [99]. However, if the REY prices become higher, this cut-off grade could be adjusted for any coals with any coal rank. Importantly, this cut-off grade could be adjusted to 800 to 900  $\mu\text{g/g}$  for coal seams with thicknesses greater than 5 m, from which relatively thick coal benches with REO higher than 1000  $\mu\text{g/g}$  (on an ash basis) are suitable for selective mining. The individual REY composition is another crucial factor. An ideal REY ore deposit should contain a diverse range of critical REY and minimize excessive elements. To assess ore quality, Seredin and Dai [20] proposed the "outlook coefficient" ( $C_{\text{outl}}$ ), which calculates the ratio of critical REY (Nd, Eu, Te, Dy, Y, Er) to excessive REY (Ce, Ho, Tm, Yb, Lu). A higher  $C_{\text{outl}}$  indicates a more promising REY ore deposit from an industrial perspective [20]. The outlook coefficient has been widely adopted and applied to the evaluation of coal-hosted REY deposits [26,60,61,100–106].

Lithium in coal has only recently been considered a recoverable metal. It began to garner significant attention and research interest in 2008 [107]. When the lithium content in coal exceeds a certain threshold, it can form a lithium deposit co-occurring with coal, categorized as a sedimentary lithium deposit. However, due to lithium's low atomic number and diverse modes of occurrence, it is one of the most challenging elements to study in coal [57,64,65,108,109]. Based on previous research and the characteristics of coal-associated metal deposits, a cut-off grade of 800  $\mu\text{g/g}$  ( $\text{Li}_2\text{O}$ , on a high-temperature ash basis) was proposed by Zhao et al. [107] as a lithium cut-off grade for recovery. In China, coal-associated lithium deposits are primarily distributed in the Carboniferous-Permian strata of North China (e.g., Jungar and Qinshui basins [18,42,66,110,111]), with a smaller portion found in the southern regions of China (e.g., Caotang Coal Mine in Sichuan Basin [112]); on the other hand, a large proportion of coals in China have

concentrations [27,41,104,113–115] that are close to those in the common coals worldwide, as proposed by Ketris and Yudovich [116].

A number of researchers have investigated the petrology, mineralogy, and geochemistry of the No. 6 coal and No. CP2 Coal from the Jungar and Daqingshan Coalfields, respectively, in Inner Mongolia [25,35,36,53–56,82,83,95–97,117–120]. The Jungar Coalfield includes the representative coal mines of Heidaigou, Haerwusu, and Guanbanwusu; the Daqingshan Coalfield includes Hailiushu, Datanhao, and Adaohai Mines.

### 5.1. Critical Metals in the Coals from the Heidaigou Mine, Jungar Coalfield

Petrologically, vitrinite reflectance from the No. 6 coal (0.58% Rr) indicates a high volatile C bituminous coal rank based on ASTM standard D388-12 (2012) [121]. Dai et al. [53,54] conducted a detailed investigation on the macerals of this coal. The inertinite and liptinite average contents are 37.4% and 7.1%, respectively. Vitrinites in this coal are primarily collodetrinite and collotelinite, although corpogelinite may predominate (up to 22.9%) in certain instances [53]. Semifusinite and inertodetrinite are the primary inertinites, with macrinite content sometimes being higher and distributed within collodetrinite. The liptinite content ranges from 2.3% to 10.8%, and liptinites are primarily sporinite and cutinite. Macrosporinite usually clusters, and microsporinite is primarily found within collodetrinite. Cutinite is predominantly thick-walled, but thin-walled cutinite is also present, primarily lining the vitrinite borders [54].

The coal's mineralogical composition can be divided into four distinct parts from bottom to top [54]. The lowest part primarily contains kaolinite, comprising approximately 21 vol.% of the mineral content (on a maceral-free basis). The second part is predominantly kaolinite (11.4%), with smaller amounts of boehmite (3.3%), pyrite, and a trace of goethite (Figure 2). The EDS data of boehmite show that Al and O contents are 49.2–57.5% and 44.4–49.7%, respectively (six test points on each photo). Boehmite is significantly enriched in the middle part, reaching an average content of ~12 vol.% (Figure 2). This high boehmite concentration is unique, as such high levels have not been observed in other coals worldwide. Kaolinite is the second most abundant mineral in this part, with an average of 4.1%. The uppermost part of the seam is characterized by a high quartz content, reaching 16.4%, and the modes of occurrence of quartz indicate that it likely originated from eroded areas of the coal basin [113,122–126].

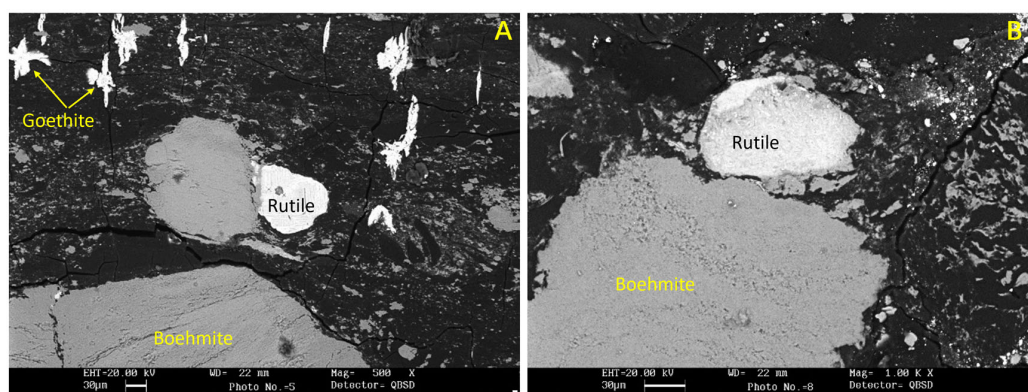


**Figure 2.** Minerals in the No. 6 coal from the Heidaigou mine, Jungar Coalfield. (A) Boehmite, goethite, and rutile; (B) boehmite and rutile. SEM back-scattered electron images.

Although the average of gallium in the entire coal seam of the Heidaigou Mine is 44.8  $\mu\text{g/g}$ , the average gallium concentration in the major minable benches of the No. 6 coal is 51.9  $\mu\text{g/g}$ , exceeding both Chinese industrial standards (30  $\mu\text{g/g}$ , whole coal basis) and the cut-off grade (50  $\mu\text{g/g}$ , ash basis) proposed by Dai et al. [55]. The major

minable benches account for a significant portion of the coal bed, representing 81.9% of the total thickness. The No. 6 coal's Ga concentration is significantly higher than that of common Chinese, US, Turkish, UK, and most global coals, as reported by Dai et al. [9], Finkelman [127], Palmer [128], and Ketris and Yudovich [116], respectively. The presence of such high gallium in such a super-thick coal bed is rare globally [53,54]. Gallium is enriched in the high-temperature (550 °C) ashes of the coal benches in the Heidaigou Mine [54]. The average Ga concentration in high-temperature ashes of the main workable benches reaches 89.2 µg/g, and 81.8 µg/g in ashes from the entire coal seam. In some ashes, gallium enrichment is significantly enriched, reaching up to 178 µg/g [54]. Dai et al. [92] reported gallium concentrations of 99.1 µg/g in fly ash and 28.7 µg/g in bottom ash from the Jungar Power Plant. The estimated fly ash to bottom ash yield ratio from this plant is approximately 9:1 [92]. The high gallium content in No. 6 coal is primarily attributed to the significant enrichment of boehmite, which contains an average gallium concentration of 900 µg/g. Boehmite constitutes an average of 6.1 vol. % of the entire coal seam and 7.5% in the main minable benches [53] in the Heidaigou mine. It originated from bauxite in the weathered crust of the Benxi Formation, which was exposed to the north coal basin during peat deposition. An estimation by Dai et al. [54] shows that No. 6 coal in the Heidaigou Mine holds ensured gallium reserves of up to 63,000 tons, making it a super-large Al-Ga ore deposit. The unique paleogeography of the Jungar Coalfield (thick coal seams, sediment-source regions, sedimentary environments, as described by Dai et al. [53,56]) and the unusual gallium host (mainly boehmite) in the coal indicate that this deposit is unparalleled globally [21]. Additionally, rare earth elements are also found in large amounts in raw coals and their high-temperature ashes in the laboratory. The concentration of total REEs is 255 µg/g and 830 µg/g in the main minable raw coal benches and their laboratory high-temperature ashes, respectively [54]. Given that Al is the dominant component of boehmite, aluminum and REEs in No.6 Coal are also available and valuable resources and should be co-recovered with Ga [54].

### 5.2. Critical Metals in the Coals from the Haerwusu Mine, Jungar Coalfield

The average vitrinite reflectance of the Haerwusu No. 6 coal is 0.57%, similar to that of the Heidaigou coals and also indicating a high volatile bituminous coal according to the ASTM Standard D388-12 [121]. The Haerwusu coal exhibits a lower vitrinite content (34%) and is significantly enriched in inertinite (46%) [56] compared to those in the Heidaigou coals in the Jungar Coalfield. Semifusinite, inertodetrinite, and macrinite are the primary inertinite macerals (Figure 3), while collodetrinite, telinite, and collotelinite dominate the vitrinite component. The liptinite macerals, including sporinite, cutinite, resinite, suberinite, and liptodetrinite (in trace amounts), are present in both coals [53,56]. As with the No. 6 coal in the Heidaigou mine, the No. 6 coal in Haerwusu mainly contains boehmite and kaolinite (Figure 4B) and traces of pyrite (Figure 4B), with the first being the dominant mineral in the middle part of coal seam [56]. Boehmite was also derived from bauxite in the weathered surface (Benxi Formation) in the sediment-source region.

The No. 6 coal is rich in Al<sub>2</sub>O<sub>3</sub> (8.89%), Li (116 µg/g), Ga (18 µg/g), Zr (268 µg/g), and REEs (172 µg/g); moreover, this coal is rich in toxic elements F (286 µg/g), Se (6.1 µg/g), Pb (30 µg/g), and Th (17 µg/g) [56]. Aluminum dominantly occurs in boehmite, and to a lesser extent, kaolinite. Statistical analysis, e.g., high correlation coefficients of the Li-ash, Li-Al<sub>2</sub>O<sub>3</sub>, and Li-SiO<sub>2</sub> pairs, indicate that Li mainly occurs in aluminosilicates in the No. 6 coal. Gallium mainly occurs in boehmite based on XRD and SEM-EDS analyses [58]. Based on sequential chemical extraction, the method that has successfully been applied to the investigations of modes of occurrence of elements in coal [124,129,130], an unusual occurrence is the presence of fluorine within the organic matter [56]. Typically, fluorine in

coal, which has attracted much attention due to its toxicity to human health [8,10,131,132], is linked to silicates and, to a lesser extent, phosphates, carbonates, and fluorite [45,69,133]. Selenium and lead are primarily found in epigenetic clausthalite, appearing as fracture fillings, similar to those reported by several researchers [21,68,134–136]. As investigated by Dai et al. [56], the abundant REEs in No. 6 Coal are believed to have originated from bauxite of the Benxi Formation and from adjacent partings within the coal seam through groundwater leaching during the late stage of peat accumulation or the diagenetic stage. Relative to heavy REEs, light REEs are more susceptible to leaching from partings and subsequent incorporation into the organic matter, resulting in a higher LREE-to-HREE ratio in coal benches than in their corresponding overlying partings. A similar phenomenon has also been observed in the Late Permian coals in the Fusui Coalfield, Guangxi Province [72], and the Late Permian coals in the Huayingshan Coalfield, Sichuan Province [137], both in southern China. However, elevated concentrations of REEs in some coals or non-coal horizons in coal-bearing sequences were derived from volcanic ashes, which were subsequently subjected to hydrothermal solutions [138–145].

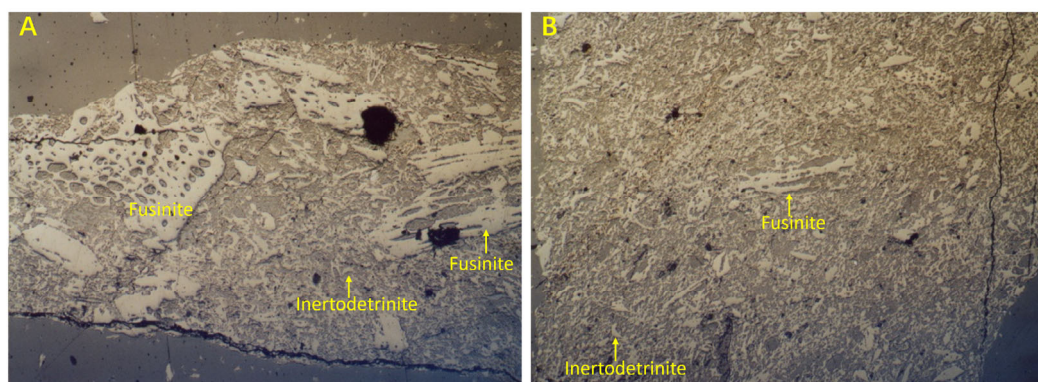


**Figure 3.** Fusinite and inertodetrinite in the No. 6 Coal from the Haerwusu mine, Jungar Coalfield, using reflected light and oil immersion. (A): Fusinite and inertodetrinite; (B) Fusinite and inertodetrinite. The width of the photo is 500  $\mu\text{m}$ .

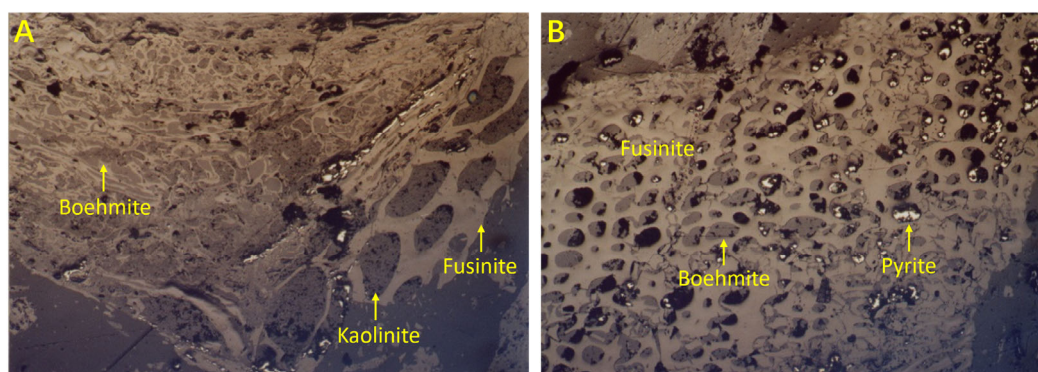


**Figure 4.** Boehmite, kaolinite, and pyrite in the No. 6 Coal from the Haerwusu mine, Jungar Coalfield, using reflected light. (A) Boehmite and kaolinite in the fusinite cells. (B) Boehmite and pyrite in the fusinite cells. The width of the photo is 500  $\mu\text{m}$ .

### 5.3. Critical Metals in the Coals from the Guanbanwusu Mine, Jungar Coalfield

The Guanbanwusu Mine is situated to the north of the Heidaigou Mine. The No. 6 Coal within the Guanbanwusu Mine exhibits a low rank ( $R_r = 0.56\%$ ), comparable to that found in the Heidaigou and Haerwusu Mines. Petrologically, the coal's inertinite content (56.7%) surpasses its vitrinite content (31.0%) [55]. The coal's mineral composition is predominantly represented by kaolinite, boehmite, and chlorite, with varying proportions of calcite, ankerite, siderite, and goyazite. Boehmite, goyazite, and a portion of the

kaolinite originated from the bauxite present in the weathered surface of the erosional region, as evidenced by their modes of occurrence, which are similar to those found in the Heidaigou and Haerwusu coals [53,56]. Like many other coals [18,33,64,77,96,146–150], carbonate minerals, including ankerite, calcite, and siderite, in the Guanbanwusu coals are of authigenic origin, as evidenced by their mode of occurrence as fracture fillings.

Chlorite is not uncommon in coal and is usually found in a relatively high rank coals [32,57,133,138,151–153]. Chemically, the chlorite composition is unique in the Guanbanwusu coals because it has a composition between cookeite and chamosite [55]. The modes of occurrence of chlorite primarily occur as cell fillings, further suggesting an authigenic formation, likely formed from hydrothermal solutions [55]. However, chlorite has not been reported in the Haerwusu and Heidaigou coals [53,56].

When compared with other Chinese and worldwide hard coals, the Guanbanwusu coal is significantly enriched in  $\text{Al}_2\text{O}_3$ ,  $\text{P}_2\text{O}_5$ , Li, Ga, and Sr, with respective concentrations of 9.34%, 0.126%, 175  $\mu\text{g/g}$ , 13  $\mu\text{g/g}$ , and 700  $\mu\text{g/g}$  (whole coal basis) [55]. The notably lower  $\text{SiO}_2/\text{Al}_2\text{O}_3$  ratio of 0.74 is a direct consequence of the higher abundances of boehmite and goyazite in the coal. Goyazite acts as the primary mineral hosting  $\text{P}_2\text{O}_5$  and Sr. Lithium in this coal is primarily associated with chlorite (exhibiting similarities to cookeite), kaolinite, and potentially, to a lesser extent, illite. Some studies also showed that Li in coal mainly occurs in clay minerals, i.e., chlorite and kaolinite [25,32,42,52,57,64,67,103,108,109,112]. Gallium in the coal is predominantly concentrated within goyazite. Rare earth elements and yttrium (REY) exhibit a dual affinity, associating with both organic and inorganic components. They are primarily concentrated within goyazite-group minerals, with additional occurrences in boehmite and organic matter [55]. Most coal seams and partings exhibit either L-type or H-type REY enrichment patterns, directly attributable to the weathered bauxite source region or groundwater leaching, respectively. The abundance of  $\text{Al}_2\text{O}_3$ , Ga, REY, and potentially Li in the Guanbanwusu coals, mirroring those found in the Jungar and Daqingshan Coalfields, signifies their potential as industrially valuable metals that are recoverable from coal combustion residues.

#### 5.4. Critical Metals in the Coals from the Laosangou Mine, Jungar Coalfield

The Laosangou Mine is located to the west of the Heidaigou, Haerwusu, and Guanbanwusu Mines of the Jungar Coalfield. Highly enriched Al, Ga, Li, and REEs in the coals from the Laosangou Mine was recently reported by [98]. The coals in the Taiyuan and Shanxi formations in the Laosangou area exhibit a notable co-enrichment of Al-Li-Ga and Nb-Ta-Zr-Hf assemblages [98]. Notably, Li, Ga, and Zr concentrations throughout the coal seam as well as Nb and Ta concentrations in specific sections of the main recoverable No. 6 coal seam reach levels suitable for industrial utilization. This highlights their significant metallogenic potential and economic value. The average ash-based content of  $\text{Al}_2\text{O}_3$  in the coal is 48.7%, significantly exceeding the industrial recovery standard of 40% for  $\text{Al}_2\text{O}_3$ , as proposed by [55]. The average ash-based content of  $\text{Li}_2\text{O}$  in the entire No. 6 coal seam is 0.13%, surpassing the cut-off grade of 0.08% for Li recovery from coal, as proposed by Zhao et al. [107]. Moreover, the ash-based content range of  $\text{Li}_2\text{O}$  in the lower volcanic ash tuff section of the No. 6 coal seam, approximately 5 m thick (583–588 cm), is 0.24–0.33%, with an average of 0.28% [98], exceeding the industrial recovery standard of 0.2% for associated lithium oxide ( $\text{Li}_2\text{O}$ ) specified in the “Geological Exploration Code for Rare Metal Minerals”. The average ash-based content of Ga in the entire No. 6 coal seam is 139  $\mu\text{g/g}$ , and that of  $\text{ZrO}_2$  is 2041  $\mu\text{g/g}$  [98], both meeting their respective industrial recovery standards. In some specific layers of the No. 6 coal seam, the ash-based content of  $\text{Nb}_2\text{O}_5$  reaches 315  $\mu\text{g/g}$ , meeting its industrial recovery standard. The carrier minerals for aluminum are boehmite and kaolinite. Lithium is hosted in kaolinite and chlorite in

the coal, while kaolinite and boehmite are the major carriers of gallium in the coal of the study area.

The enrichment of Al, Ga, and Li in the coal-bearing Taiyuan and Shanxi formations is a product of complex geological processes [98]. Initially, the weathering and denudation of Mesoproterozoic moyite in the Yinshan Oldland provided a primary source for Al, Ga, and Li. Terrigenous detritus originating from this source was initially enriched in the weathering crust of the Upper Carboniferous Benxi Formation, situated in the northeastern part of the basin, serving as a direct material source for Al, Ga, and Li enrichment in the coal-bearing sequences. Subsequently, fluid activity and water/rock interactions played a pivotal role. Al, Ga, and Li migrated alongside groundwater, eventually being deposited and enriched within the coal-bearing sequence. Finally, the introduction of Li, Ga, Nb, and Ta-rich intermediate-felsic alkaline volcanic ash, in conjunction with the migration of hydrothermal fluids, led to secondary enrichment of these elements in the studied coals during the coalification process [98].

##### 5.5. Critical Metals in the Coals from the Adaohai Mine, Daqingshan Coalfield

The CP2 coal seam, the primary target for mining at the Adaohai Mine in the Daqingshan Coalfield of Inner Mongolia, exhibits a higher rank ( $R_o = 1.58\%$ ) than those in the same coals in neighboring mines in the Daqingshan Coalfield [84,95,97]. This elevated rank is a result of igneous intrusions that occurred during the late Jurassic to early Cretaceous ages. Elevated coal ranks caused by igneous intrusions have also been reported in a number of other areas around the world [75,78,154,155], but it seems that concentrations of critical elements in these hydrothermally altered coals were not highly enough to be recovered [113,156,157]. The CP2 coal contains a higher inertinite content, i.e., 35.3%. Compared with the common Chinese and world coals, the CP2 coal is enriched in  $Al_2O_3$  (10.75%, whole coal basis), Ga (16.3  $\mu\text{g/g}$ ), and Zr (446  $\mu\text{g/g}$ ) and has a lower  $SiO_2/Al_2O_3$  ratio (0.93) due to the higher proportions of diaspore, boehmite, and gorceixite in the coal [97]. The average ash yield of the coal seam is 25.1%. The average concentration of  $Al_2O_3$  and Ga in the coal ash is 42.8% and 65  $\mu\text{g/g}$ , respectively, reaching their cut-off grade (40% and 50  $\mu\text{g/g}$ , respectively). The major hosts of Ga are diaspore and kaolinite. The coals exhibit an enrichment in light rare earth elements (LREEs) and a significant fractionation of LREEs and HREEs, with an average  $(La/Yb)_N$  value of 8.71. Heavy REEs in the coals demonstrate a stronger organic affinity compared to LREEs. The mineral assemblage of the CP2 coal includes hydrodioxides (e.g., boehmite and diaspore), phosphate minerals (e.g., gorceixite), carbonate minerals (e.g., dolomite, calcite, and siderite), and clay minerals (e.g., kaolinite and ammonian-illite) [96,111,112]. The hydrodioxides and phosphate minerals as mentioned above originated from oxidized bauxite in the erosional areas during peat deposition. In contrast to diaspore, which originated from gibbsite dehydrated by the heat of igneous intrusions, gorceixite may have formed at an earlier stage [158–160]. Ammonian illite likely formed at a relatively high temperature through the interaction of kaolinite with N released from the organic matter of the coal during the metamorphism induced by the igneous intrusion [82,96,161]. Calcite and dolomite, occurring as epigenetic cell and fracture fillings, probably derived from igneous fluids [96].

The Adaohai Mine is situated approximately 50 km southwest of the intrusion. The Datanhao Mine is located between the Hailiushu and Adaohai Mines; the latter two mines are separated by a distance of about 10 km [82]. As proximity to the intrusion increases, so does vitrinite reflectance (from 0.84% to 1.17% to 1.58%), but volatile matter yield decreases (from 44.57% to 31.31% to 19.60%) in the three coal mines mentioned above [83,84,95,97]. The coals in the Hailiushu mine, which is located at the westernmost area of the coalfield, exhibits the most negative  $\delta^{13}\text{C}$  values for organic matter (from  $-24.8\%$  to  $-23.5\%$ , mean of

−24.3‰). Conversely, as distance from the intrusion diminishes, the carbon isotope values of the organic matter of coals from the Datanhao Mine vary from −24.8‰ to −23.5‰ (mean of −24.2‰). The easternmost Adaohai coals in the Daqingshan Coalfield display  $\delta^{13}\text{C}$  values of organic matter between −23.8‰ and −22.8‰ (mean of −23.3‰), approximately 1‰ more positive than those found in the coals from the Datanhao and Hailiushu Mines. The variation in  $\delta^{13}\text{C}$  values of organic matter is not solely attributed to macerals but also to the loss of volatiles that are rich in  $^{12}\text{C}$ , resulting from the heat generated by the igneous intrusions in the coalfield. As previously reported by other researchers [6,162–165], the  $\delta^{13}\text{C}$  variation of organic matter in coal is caused by several reasons, such as coal-forming plants, sedimentary environments, paleoclimate, and rank advance.

The hypothesis proposed by Dai et al. [97], i.e., the coal was subjected to igneous intrusion, was corroborated by Rock-Eval analysis of the organic matter [96], which revealed an increase in the average Tmax value in the order of Hailiushu, Datanhao, and Adaohai coals. Additionally, fracture-filling and/or cleat-filling carbonate minerals were more commonly prevalent in the coals of Adaohai than those of the Datanhao Mine. The  $\delta^{13}\text{C}_{\text{PDB}}$  values (ranging from −14.2‰ to −1.7‰) and  $\delta^{18}\text{O}_{\text{PDB}}$  (ranging from −16.9‰ to −7.0‰) of these veined carbonate minerals collectively suggest a precipitation of hydrothermal solutions [96], which originated from the igneous intrusion and were implied by the high  $^{87}\text{Sr}/^{86}\text{Sr}$  values (varying from 0.711392 to 0.717643) of carbonates within the hydrothermal solution-affected coals [96].  $^{87}\text{Sr}/^{86}\text{Sr}$  values have also been successfully used as indicators for depositional environments [47,166] and sources of critical element Ge in coal [47].

## 6. Benefits of Recovery of Critical Metals from Coal Combustion By-Products

The ensured coal reserves in the Jungar Coalfield are estimated at 58.2 billion tons. High-aluminum coal reserves, accounting for 26.7 billion tons, are recoverable from this region, with an annual mining capacity of approximately 100 million tons. Consequently, the annual coal combustion byproduct from this mining activity is estimated at 2 million tons. Therefore, extracting critical elements from the Jungar coal ash offers a number of important advantages. First, it can ensure a possible stable supply of critical elements of Al, Ga, Li, rare earth elements, and possibly Zr and Nb, bolstering national security and economic development. Second, it may mitigate the challenges associated with developing new conventional metalliferous mines by utilizing an existing coal combustion byproduct that is highly rich in these critical metals [167], thereby significantly reducing infrastructure and mining costs. Third, the energy-intensive grinding process is bypassed, as fly ash is already finely particulate. Forth, traditional coal mining and utilization's environmental consequences, including dust emissions and the risk of slurry impoundment breaches, could be minimized. For example, the leaching of toxic elements (e.g., F, Pb, Hg, and As) from fly ash into ground water, a common issue with tailings [168,169], could be prevented. Finally, the financial and environmental burdens of coal combustion product disposal are alleviated through the co-recovery of several critical elements. These economic and environmental benefits make Jungar and possibly Daqingshan coals and their coal combustion byproducts an attractive source of critical elements, particularly for China, a country with substantial coal consumption [170].

## 7. Conclusions

Overall, compared with conventional critical metal deposits, coal-hosted Al-Ga-Li-REE deposits have the following characteristics: (1) they were discovered, explored, and developed relatively late, belonging to a new type of critical metal deposit; (2) these deposits have huge resources/reserves, often forming large or super-large critical metal deposits;

(3) these deposits are characterized by the co-enrichment of multiple metals, providing conditions for the co-recovery of various metals; (4) the stratigraphic position of these deposits is stable in both thickness and space, and the coal structure is relatively simple, making exploration and development relatively easy and cost-effective.

To better develop and utilize these deposits, the following work should be emphasized and carried out in the future: (1) Work should focus on the joint exploration and development of coal resources and critical metal resources to reduce the cost of exploration and development of coal-hosted critical metals and shorten the exploration and development cycle. (2) Since REEs are highly enriched in these deposits but have not been developed and utilized, in addition to gallium, aluminum, and lithium, the development and utilization of REEs in coal and fly ash should also be strengthened to improve resource utilization efficiency and reduce the cost of critical metal development. (3) Toxic elements such as fluorine and lead are enriched in these deposits, and their harm to the environment and health should be considered during the extraction and development of critical metals, particularly their concentrations, modes of occurrence, and migration during critical metal extraction from coal ashes. A high-efficiency technology for controlling their adverse effects on environments should be developed. (4) Further research should be conducted on the mineralization theory of critical elements in order to provide basic data on coal geochemistry and coal mineralogy for regional geological evolution but also provide references and directions for the search and development of similar ore deposits in other areas.

**Author Contributions:** Conceptualization, Y.Z. and W.Z.; methodology, X.L.; software and validation, W.Z.; investigation, Y.Z., X.L. and W.Z.; data curation, Y.Z. and W.Z.; writing—original draft preparation, Y.Z.; writing—review and editing, W.Z. and X.L.; visualization, W.Z.; supervision, Y.Z.; administration, Y.Z.; funding acquisition, Y.Z. All authors have read and agreed to the published version of the manuscript.

**Funding:** This research was financially supported by the Technological Innovation Projects of Shenhua Geological Exploration Co., Ltd. (No. GSKJ-24-124).

**Data Availability Statement:** The original contributions presented in the study are included in the article Materials.

**Acknowledgments:** We wish to acknowledge Yu Liu from China University of Mining and Technology (Beijing) for the help during the manuscript preparation.

**Conflicts of Interest:** The authors declare no conflicts of interest. Yanbo Zhang, Xiangyang Liu, Wei Zhao are employees of Shenhua Geological Exploration Co., Ltd. The paper reflects the views of the scientists and not the company.

## References

1. Finkelman, R.B.; Dai, S.F.; French, D. The importance of minerals in coal as the hosts of chemical elements: A review. *Int. J. Coal Geol.* **2019**, *212*, 103251. [[CrossRef](#)]
2. Dai, S.F.; Finkelman, R.B.; French, D.; Hower, J.C.; Graham, I.T.; Zhao, F.H. Modes of occurrence of elements in coal: A critical evaluation. *Earth-Sci. Rev.* **2021**, *222*, 103815. [[CrossRef](#)]
3. Ward, C.R. Analysis and significance of mineral matter in coal seams. *Int. J. Coal Geol.* **2002**, *50*, 135–168. [[CrossRef](#)]
4. Ward, C.R. Analysis, origin and significance of mineral matter in coal: An updated review. *Int. J. Coal Geol.* **2016**, *165*, 1–27. [[CrossRef](#)]
5. Dai, S.F.; Ren, D.; Tang, Y.G.; Yue, M.; Hao, L.M. Concentration and distribution of elements in Late Permian coals from western Guizhou Province, China. *Int. J. Coal Geol.* **2005**, *61*, 119–137. [[CrossRef](#)]
6. Wang, R.; Dai, S.; Spiro, B.F.; Nechaev, V.P.; French, D.; Graham, I.T.; Zhou, M.; Liu, J.; Di, S.; Tian, X. Multi-stage hydrothermal activity affecting the early Jurassic K7 coal seam from the Gaosheng coal Mine, Sichuan Basin, southwest China: Evidence from whole-rock geochemistry and C-O-Sr isotopes in authigenic carbonates. *J. Asian Earth Sci.* **2025**, *278*, 106410. [[CrossRef](#)]
7. Zhou, M.; Dai, S.; Wang, X.; Zhao, L.; Nechaev, V.P.; French, D.; Graham, I.T.; Zheng, J.; Wang, Y.; Dong, M. Critical element (Nb-Ta-Zr-Hf-REE-Ga-Th-U) mineralization in Late Triassic coals from the Gaosheng Mine, Sichuan Basin, southwestern China:

- Coupled effects of products of sediment-source-region erosion and acidic water infiltration. *Int. J. Coal Geol.* **2022**, *262*, 104101. [[CrossRef](#)]
8. Dai, S.F.; Li, W.W.; Tang, Y.G.; Zhang, Y.; Feng, P. The sources, pathway, and preventive measures for fluorosis in Zhijin County, Guizhou, China. *Appl. Geochem.* **2007**, *22*, 1017–1024. [[CrossRef](#)]
  9. Dai, S.F.; Ren, D.Y.; Chou, C.L.; Finkelman, R.B.; Seredin, V.V.; Zhou, Y.P. Geochemistry of trace elements in Chinese coals: A review of abundances, genetic types, impacts on human health, and industrial utilization. *Int. J. Coal Geol.* **2012**, *94*, 3–21. [[CrossRef](#)]
  10. Dai, S.F.; Ren, D.Y.; Ma, S.M. The cause of endemic fluorosis in western Guizhou Province, Southwest China. *Fuel* **2004**, *83*, 2095–2098. [[CrossRef](#)]
  11. Finkelman, R.B.; Gross, P.M.K. The types of data needed for assessing the environmental and human health impacts of coal. *Int. J. Coal Geol.* **1999**, *40*, 91–101. [[CrossRef](#)]
  12. Dai, S.F.; Zeng, R.S.; Sun, Y.Z. Enrichment of arsenic, antimony, mercury, and thallium in a Late Permian anthracite from Xingren, Guizhou, Southwest China. *Int. J. Coal Geol.* **2006**, *66*, 217–226. [[CrossRef](#)]
  13. Dai, S.F.; Finkelman, R.B. Coal as a promising source of critical elements: Progress and future prospects. *Int. J. Coal Geol.* **2018**, *186*, 155–164. [[CrossRef](#)]
  14. Dai, S.F.; Yan, X.Y.; Ward, C.R.; Hower, J.C.; Zhao, L.; Wang, X.B.; Zhao, L.X.; Ren, D.Y.; Finkelman, R.B. Valuable elements in Chinese coals: A review. *Int. Geol. Rev.* **2018**, *60*, 590–620. [[CrossRef](#)]
  15. Dai, S.F.; Wang, X.B.; Seredin, V.V.; Hower, J.C.; Ward, C.R.; O'Keefe, J.M.K.; Huang, W.H.; Li, T.; Li, X.; Liu, H.D.; et al. Petrology, mineralogy, and geochemistry of the Ge-rich coal from the Wulantuga Ge ore deposit, Inner Mongolia, China: New data and genetic implications. *Int. J. Coal Geol.* **2012**, *90*, 72–99. [[CrossRef](#)]
  16. Seredin, V.V. Rare earth element-bearing coals from the Russian Far East deposits. *Int. J. Coal Geol.* **1996**, *30*, 101–129. [[CrossRef](#)]
  17. Seredin, V.V. Anomalous trace elements contents in the Spetsugli germanium deposit (Pavlovka brown coal deposit) southern Primorye: Communication 1. Antimony. *Lithol. Miner. Resour.* **2003**, *38*, 154–161. [[CrossRef](#)]
  18. Hou, Y.J.; Dai, S.F.; Nechaev, V.P.; Finkelman, R.B.; Wang, H.D.; Zhang, S.W.; Di, S.B. Mineral matter in the Pennsylvanian coal from the Yangquan Mining District, northeastern Qinshui Basin, China: Enrichment of critical elements and a Se-Mo-Pb-Hg assemblage. *Int. J. Coal Geol.* **2023**, *266*, 104178. [[CrossRef](#)]
  19. Seredin, V.V. From coal science to metal production and environmental protection: A new story of success Commentary. *Int. J. Coal Geol.* **2012**, *90*, 1–3. [[CrossRef](#)]
  20. Seredin, V.V.; Dai, S.F. Coal deposits as potential alternative sources for lanthanides and yttrium. *Int. J. Coal Geol.* **2012**, *94*, 67–93. [[CrossRef](#)]
  21. Seredin, V.V.; Finkelman, R.B. Metalliferous coals: A review of the main genetic and geochemical types. *Int. J. Coal Geol.* **2008**, *76*, 253–289. [[CrossRef](#)]
  22. Dai, S.F.; Wang, P.P.; Ward, C.R.; Tang, Y.G.; Song, X.L.; Jiang, J.H.; Hower, J.C.; Li, T.; Seredin, V.V.; Wagner, N.J.; et al. Elemental and mineralogical anomalies in the coal-hosted Ge ore deposit of Lincang, Yunnan, southwestern China: Key role of N<sub>2</sub>-CO<sub>2</sub>-mixed hydrothermal solutions. *Int. J. Coal Geol.* **2015**, *152*, 19–46. [[CrossRef](#)]
  23. Hower, J.C.; Qian, D.L.; Briot, N.J.; Hood, M.M.; Eble, C.F. Mineralogy of a rare earth element-rich Manchester coal lithotype, Clay County, Kentucky. *Int. J. Coal Geol.* **2020**, *220*, 103413. [[CrossRef](#)]
  24. Arbuzov, S.I.; Chekryzhov, I.Y.; Verkhoturov, A.A.; Spears, D.A.; Melkiy, V.A.; Zarubina, N.V.; Blokhin, M.G. Geochemistry and rare-metal potential of coals of the Sakhalin coal basin, Sakhalin island, Russia. *Int. J. Coal Geol.* **2023**, *268*, 104197. [[CrossRef](#)]
  25. Jiu, B.; Huang, W.H.; Spiro, B.; Hao, R.L.; Mu, N.A.; Wen, L.; Hao, H.D. Distribution of Li, Ga, Nb, and REEs in coal as determined by LA-ICP-MS imaging: A case study from Jungar coalfield, Ordos Basin, China. *Int. J. Coal Geol.* **2023**, *267*, 104184. [[CrossRef](#)]
  26. Palozzi, J.; Bailey, J.G.; Tran, Q.A.; Stanger, R. A characterization of rare earth elements in coal ash generated during the utilization of Australian coals. *Int. J. Coal Prep.* **2023**, *43*, 2106–2135. [[CrossRef](#)]
  27. Shen, M.L.; Dai, S.F.; Nechaev, V.P.; French, D.; Graham, I.T.; Liu, S.D.; Chekryzhov, I.Y.; Tarasenko, I.A.; Zhang, S.W. Provenance changes for mineral matter in the latest Permian coals from western Guizhou, southwestern China, relative to tectonic and volcanic activity in the Emeishan Large Igneous Province and Paleo-Tethys region. *Gondwana Res.* **2023**, *113*, 71–88. [[CrossRef](#)]
  28. Wu, J.Y.; Yang, Y.; Tou, F.Y.; Yan, X.Y.; Dai, S.F.; Hower, J.C.; Saikia, B.K.; Kersten, M.; Hochella, M.F. Combustion conditions and feed coals regulating the Fe- and Ti-containing nanoparticles in various coal fly ash. *J. Hazard. Mater.* **2023**, *445*, 130482. [[CrossRef](#)]
  29. Zhang, Z.H.; Lv, D.W.; Hower, J.C.; Wang, L.J.; Shen, Y.Y.; Zhang, A.C.; Xu, J.C.; Gao, J. Geochronology, mineralogy, and geochemistry of tonsteins from the Pennsylvanian Taiyuan Formation of the Jungar Coalfield, Ordos Basin, North China. *Int. J. Coal Geol.* **2023**, *267*, 104183. [[CrossRef](#)]
  30. Hower, J.C.; Warwick, P.D.; Scanlon, B.R.; Reedy, R.C.; Childress, T.M. Distribution of rare earth and other critical elements in lignites from the Eocene Jackson Group, Texas. *Int. J. Coal Geol.* **2023**, *275*, 104302. [[CrossRef](#)]
  31. Arnold, B.J. A review of element partitioning in coal preparation. *Int. J. Coal Geol.* **2023**, *274*, 104296. [[CrossRef](#)]

32. Di, S.B.; Dai, S.F.; Nechaev, V.P.; French, D.; Graham, I.T.; Zhao, L.; Finkelman, R.B.; Wang, H.D.; Zhang, S.W.; Hou, Y.J. Mineralogy and enrichment of critical elements (Li and Nb-Ta-Zr-Hf-Ga) in the Pennsylvanian coals from the Antaibao Surface Mine, Shanxi Province, China: Derivation of pyroclastics and sediment-source regions. *Int. J. Coal Geol.* **2023**, *273*, 104262. [[CrossRef](#)]
33. Yang, P.; Dai, S.F.; Nechaev, V.P.; Song, X.L.; Chekryzhov, I.Y.; Tarasenko, I.A.; Tian, X.; Yao, M.D.; Kang, S.; Zheng, J.T. Modes of occurrence of critical metals (Nb-Ta-Zr-Hf-REY-Ga) in altered volcanic ashes in the Xuanwei Formation, eastern Yunnan Province, SW China: A quantitative evaluation based on sequential chemical extraction. *Ore Geol. Rev.* **2023**, *160*, 105617. [[CrossRef](#)]
34. Yang, T.Y.; Shen, Y.L.; Lu, L.; Jin, J.; Huang, W.; Li, F.Y.; Zhang, Y.F.; Hu, J.C.; Zeng, L.J. Geological factors for the enrichment of critical elements within the Lopingian (Late Permian) coal-bearing strata in western Guizhou, Southwestern China: Constrained with whole-rock and zircon geochemistry. *Int. J. Coal Geol.* **2024**, *282*, 105617. [[CrossRef](#)]
35. Zhang, S.; Xiu, W.; Sun, B.; Liu, Q.F. Provenance of multi-stage volcanic ash recorded in the Late Carboniferous coal in the Jungar Coalfield, North China, and their contribution to the enrichment of critical metals in the coal. *Int. J. Coal Geol.* **2023**, *273*, 104265. [[CrossRef](#)]
36. Zhang, S.; Yuan, T.C.; Sun, B.; Li, L.; Ma, X.J.; Shi, S.L.; Liu, Q.F. Formation of boehmite through desilication of volcanic-ash-altered kaolinite and its retention for gallium: Contribution to enrichment of aluminum and gallium in coal. *Int. J. Coal Geol.* **2024**, *281*, 104404. [[CrossRef](#)]
37. Seredin, V.V.; Chekryzhov, I.Y. Ore Potentiality of the Vanchin Graben, Primorye, Russia. *Geol. Ore Depos.* **2011**, *53*, 202–220. [[CrossRef](#)]
38. Seredin, V.V.; Dai, S.F.; Sun, Y.Z.; Chekryzhov, I.Y. Coal deposits as promising sources of rare metals for alternative power and energy-efficient technologies. *Appl. Geochem.* **2013**, *31*, 1–11. [[CrossRef](#)]
39. Hower, J.C.; Finkelman, R.B.; Eble, C.F.; Arnold, B.J. Understanding coal quality and the critical importance of comprehensive coal analyses. *Int. J. Coal Geol.* **2022**, *263*, 104120. [[CrossRef](#)]
40. Dai, S.F.; Seredin, V.V.; Ward, C.R.; Jiang, J.H.; Hower, J.C.; Song, X.L.; Jiang, Y.F.; Wang, X.B.; Gornostaeva, T.; Li, X.; et al. Composition and modes of occurrence of minerals and elements in coal combustion products derived from high-Ge coals. *Int. J. Coal Geol.* **2014**, *121*, 79–97. [[CrossRef](#)]
41. Liu, J.J.; Dai, S.F.; Berti, D.; Eble, C.F.; Dong, M.J.; Gao, Y.; Hower, J.C. Rare Earth and Critical Element Chemistry of the Volcanic Ash-fall Parting in the Fire Clay Coal, Eastern Kentucky, USA. *Clays Clay Miner.* **2023**, *71*, 309–339. [[CrossRef](#)]
42. Zhang, W.; Zhao, L.; Wang, W.; Nechaev, V.P.; French, D.; Graham, I.; Lang, Y.B.; Li, Z.P.; Dai, S.F. Enrichment of critical metals (Li, Ga, and rare earth elements) in the early Permian coal seam from the Jincheng Coalfield, southeastern Qinshui Basin, northern China: With an emphasis on cookeite as the Li host. *Ore Geol. Rev.* **2024**, *167*, 105939. [[CrossRef](#)]
43. Dai, S.F.; Chekryzhov, I.Y.; Seredin, V.V.; Nechaev, V.P.; Graham, I.T.; Hower, J.C.; Ward, C.R.; Ren, D.Y.; Wang, X.B. Metalliferous coal deposits in East Asia (Primorye of Russia and South China): A review of geodynamic controls and styles of mineralization. *Gondwana Res.* **2016**, *29*, 60–82. [[CrossRef](#)]
44. Dai, S.F.; Liu, J.J.; Ward, C.R.; Hower, J.C.; Xie, P.P.; Jiang, Y.F.; Hood, M.M.; O’Keefe, J.M.K.; Song, H.J. Petrological, geochemical, and mineralogical compositions of the low-Ge coals from the Shengli Coalfield, China: A comparative study with Ge-rich coals and a formation model for coal-hosted Ge ore deposit. *Ore Geol. Rev.* **2015**, *71*, 318–349. [[CrossRef](#)]
45. Dai, S.F.; Seredin, V.V.; Ward, C.R.; Hower, J.C.; Xing, Y.W.; Zhang, W.G.; Song, W.J.; Wang, P.P. Enrichment of U-Se-Mo-Re-V in coals preserved within marine carbonate successions: Geochemical and mineralogical data from the Late Permian Guiding Coalfield, Guizhou, China. *Miner. Depos.* **2015**, *50*, 159–186. [[CrossRef](#)]
46. Etschmann, B.; Liu, W.H.; Li, K.; Dai, S.F.; Reith, F.; Falconer, D.; Kerr, G.; Paterson, D.; Howard, D.; Kappen, P.; et al. Enrichment of germanium and associated arsenic and tungsten in coal and roll-front uranium deposits. *Chem. Geol.* **2017**, *463*, 29–49. [[CrossRef](#)]
47. Liu, J.J.; Spiro, B.F.; Dai, S.F.; French, D.; Graham, I.T.; Wang, X.B.; Zhao, L.; Zhao, J.T.; Zeng, R.S. Strontium isotopes in high- and low-Ge coals from the Shengli Coalfield, Inner Mongolia, northern China: New indicators for Ge source. *Int. J. Coal Geol.* **2021**, *233*, 103642. [[CrossRef](#)]
48. Wei, Q.; Cui, C.N.; Dai, S.F. Organic-association of Ge in the coal-hosted ore deposits: An experimental and theoretical approach. *Ore Geol. Rev.* **2020**, *117*, 103291. [[CrossRef](#)]
49. Chitlango, F.Z.; Wagner, N.J.; Moroeng, O.M. Characterization and pre-concentration of rare earth elements in density fractionated samples from the Waterberg Coalfield, South Africa. *Int. J. Coal Geol.* **2023**, *275*, 104299. [[CrossRef](#)]
50. Dai, S.; Finkelman, R.B.; Hower, J.C.; French, D.; Graham, I.T.; Zhao, L. (Eds.) Chapter 10—Critical elements in coal. In *Inorganic Geochemistry of Coal*; Elsevier: Amsterdam, The Netherlands, 2023; pp. 235–380.
51. Willard, D.A.; Ruppert, L.F. Broadening the perspectives of sedimentary organic matter analysis to understand Earth system response to change. *Int. J. Coal Geol.* **2023**, *274*, 104281. [[CrossRef](#)]
52. Xu, F.; Qin, S.J.; Li, S.Y.; Wen, H.J.; Lv, D.W.; Wang, Q.; Kang, S. The migration and mineral host changes of lithium during coal combustion: Experimental and thermodynamic calculation study. *Int. J. Coal Geol.* **2023**, *275*, 104298. [[CrossRef](#)]

53. Dai, S.F.; Ren, D.Y.; Chou, C.L.; Li, S.S.; Jiang, Y.F. Mineralogy and geochemistry of the No. 6 coal (Pennsylvanian) in the Junger Coalfield, Ordos Basin, China. *Int. J. Coal Geol.* **2006**, *66*, 253–270. [[CrossRef](#)]
54. Dai, S.F.; Ren, D.Y.; Li, S.S. Discovery of the superlarge gallium ore deposit in Jungar, Inner Mongolia, North China. *Chin. Sci. Bull.* **2006**, *51*, 2243–2252. [[CrossRef](#)]
55. Dai, S.F.; Jiang, Y.F.; Ward, C.R.; Gu, L.D.; Seredin, V.V.; Liu, H.D.; Zhou, D.; Wang, X.B.; Sun, Y.Z.; Zou, J.H.; et al. Mineralogical and geochemical compositions of the coal in the Guanbanwusu Mine, Inner Mongolia, China: Further evidence for the existence of an Al (Ga and REE) ore deposit in the Jungar Coalfield. *Int. J. Coal Geol.* **2012**, *98*, 10–40. [[CrossRef](#)]
56. Dai, S.F.; Li, D.; Chou, C.L.; Zhao, L.; Zhang, Y.; Ren, D.; Ma, Y.W.; Sun, Y.Y. Mineralogy and geochemistry of boehmite-rich coals: New insights from the Haerwusu Surface Mine, Jungar Coalfield, Inner Mongolia, China. *Int. J. Coal Geol.* **2008**, *74*, 185–202. [[CrossRef](#)]
57. Yuan, D.E.; Wang, X.M.; Yan, D.T.; Li, J.; Li, B.Q.; Liu, B.; Liu, Z.X.; Zhang, L.W. An original set of nanometer-scale mineralogical analyses of cookeite and the implications for Li enrichment: No. 2 coal, Mengjin Mine, western Henan. *Int. J. Coal Geol.* **2024**, *283*, 104445. [[CrossRef](#)]
58. Moroeng, O.M.; Murathi, B.; Wagner, N.J. Enrichment of rare earth elements in epigenetic dolomite occurring in contact metamorphosed Witbank coals (South Africa). *Int. J. Coal Geol.* **2024**, *282*, 104405. [[CrossRef](#)]
59. Dai, S.F.; Graham, I.T.; Ward, C.R. A review of anomalous rare earth elements and yttrium in coal. *Int. J. Coal Geol.* **2016**, *159*, 82–95. [[CrossRef](#)]
60. Strzałkowska, E. Rare earth elements and other critical elements in the magnetic fraction of fly ash from several Polish power plants. *Int. J. Coal Geol.* **2022**, *258*, 104015. [[CrossRef](#)]
61. Mokoena, B.K.; Mokhahlane, L.S.; Clarke, S. Effects of acid concentration on the recovery of rare earth elements from coal fly ash. *Int. J. Coal Geol.* **2022**, *259*, 104037. [[CrossRef](#)]
62. Wang, Z.; Dai, S.; Zou, J.; French, D.; Graham, I.T. Rare earth elements and yttrium in coal ash from the Luzhou power plant in Sichuan, Southwest China: Concentration, characterization and optimized extraction. *Int. J. Coal Geol.* **2019**, *203*, 1–14. [[CrossRef](#)]
63. Liu, C.; Chang, Y.; Sun, B.; Wang, X.; Qi, F. Detrital material controlling the enrichment of critical element Li in No. 9 coal seam of the Ningwu Coalfield, northeastern Shanxi Province, China: Heavy mineral and detrital zircon constraints. *Int. J. Coal Geol.* **2024**, *294*, 104605. [[CrossRef](#)]
64. Sun, B.; Guo, Z.; Liu, C.; Kong, Y.; French, D.; Zhu, Z. Lithium isotopic composition of two high-lithium coals and their fractions with different lithium occurrence modes, Shanxi Province, China. *Int. J. Coal Geol.* **2023**, *277*, 104338. [[CrossRef](#)]
65. Sun, B.; Zeng, F.; Moore, T.A.; Rodrigues, S.; Liu, C.; Wang, G. Geochemistry of two high-lithium content coal seams, Shanxi Province, China. *Int. J. Coal Geol.* **2022**, *260*, 104059. [[CrossRef](#)]
66. Hou, Y.; Liu, D.; Zhao, F.; Zhang, S.; Zhang, Q.; Emmanuel, N.N.; Zhong, L. Mineralogical and geochemical characteristics of coal from the Southeastern Qinshui Basin: Implications for the enrichment and economic value of Li and REY. *Int. J. Coal Geol.* **2022**, *264*, 104136. [[CrossRef](#)]
67. Jiu, B.; Huang, W.; Mu, N. Mineralogy and elemental geochemistry of Permo-Carboniferous Li-enriched coal in the southern Ordos Basin, China: Implications for modes of occurrence, controlling factors and sources of Li in coal. *Ore Geol. Rev.* **2022**, *141*, 104686. [[CrossRef](#)]
68. Dai, S.F.; Yang, J.Y.; Ward, C.R.; Hower, J.C.; Liu, H.D.; Garrison, T.M.; French, D.; O’Keefe, J.M.K. Geochemical and mineralogical evidence for a coal-hosted uranium deposit in the Yili Basin, Xinjiang, northwestern China. *Ore Geol. Rev.* **2015**, *70*, 1–30. [[CrossRef](#)]
69. Dai, S.F.; Zhang, W.G.; Seredin, V.V.; Ward, C.R.; Hower, J.C.; Song, W.J.; Wang, X.B.; Li, X.; Zhao, L.X.; Kang, H.; et al. Factors controlling geochemical and mineralogical compositions of coals preserved within marine carbonate successions: A case study from the Heshan Coalfield, southern China. *Int. J. Coal Geol.* **2013**, *109*, 77–100. [[CrossRef](#)]
70. Shao, L.Y.; Zhang, P.F.; Gayer, R.A.; Chen, J.L.; Dai, S.F. Coal in a carbonate sequence stratigraphic framework: The Upper Permian Heshan Formation in central Guangxi, southern China. *J. Geol. Soc.* **2003**, *160*, 285–298. [[CrossRef](#)]
71. Dai, S.; Xie, P.; Ward, C.R.; Yan, X.; Guo, W.; French, D.; Graham, I.T. Anomalies of rare metals in Lopingian super-high-organic-sulfur coals from the Yishan Coalfield, Guangxi, China. *Ore Geol. Rev.* **2017**, *88*, 235–250. [[CrossRef](#)]
72. Dai, S.F.; Zhang, W.G.; Ward, C.R.; Seredin, V.V.; Hower, J.C.; Li, X.; Song, W.J.; Wang, X.B.; Kang, H.; Zheng, L.C.; et al. Mineralogical and geochemical anomalies of late Permian coals from the Fusui Coalfield, Guangxi Province, southern China: Influences of terrigenous materials and hydrothermal fluids. *Int. J. Coal Geol.* **2013**, *105*, 60–84. [[CrossRef](#)]
73. Dai, S.F.; Ren, D.Y.; Zhou, Y.P.; Chou, C.L.; Wang, X.B.; Zhao, L.; Zhu, X.W. Mineralogy and geochemistry of a superhigh-organic-sulfur coal, Yanshan Coalfield, Yunnan, China: Evidence for a volcanic ash component and influence by submarine exhalation. *Chem. Geol.* **2008**, *255*, 182–194. [[CrossRef](#)]
74. Dai, S.; Zheng, X.; Wang, X.; Finkelman, R.B.; Jiang, Y.; Ren, D.; Yan, X.; Zhou, Y. Stone coal in China: A review. *Int. Geol. Rev.* **2018**, *60*, 736–753. [[CrossRef](#)]

75. Wang, N.; Esterle, J.S.; Rodrigues, S.; Hower, J.C.; Dai, S. Insights on the regional thermal evolution from semianthracite petrology of the Fengfeng coalfield, China. *Int. J. Coal Geol.* **2024**, *290*, 104548. [[CrossRef](#)]
76. Xu, N.; Zhu, W.; Wang, R.; Li, Q.; Wang, Z.; Finkelman, R.B. Application of self-organizing maps to coal elemental data. *Int. J. Coal Geol.* **2023**, *277*, 104358. [[CrossRef](#)]
77. Shang, N.D.; Liu, J.J.; Han, Q.C.; Jia, R.K.; Zhao, S.M. Mineralogy and geochemistry of the Middle Jurassic coal from the Hexi Mine, Shenfu Mining Area, Ordos Basin: With an emphasis on genetic indications of siderite. *Int. J. Coal Geol.* **2023**, *279*, 104384. [[CrossRef](#)]
78. Wang, N.; Dai, S.; Esterle, J.; Moore, T.; Zhao, L. Geochemical and mineralogical responses to thermal alteration by an igneous intrusion in the Dashucun Coal Mine of the Fengfeng coalfield, Hebei, North China. *Appl. Geochem.* **2024**, *160*, 105877. [[CrossRef](#)]
79. Dai, S.; Ward, C.R.; Graham, I.T.; French, D.; Hower, J.C.; Zhao, L.; Wang, X. Altered volcanic ashes in coal and coal-bearing sequences: A review of their nature and significance. *Earth-Sci. Rev.* **2017**, *175*, 44–74. [[CrossRef](#)]
80. Dai, S.F.; Wang, X.B.; Zhou, Y.P.; Hower, J.C.; Li, D.H.; Chen, W.M.; Zhu, X.W.; Zou, J.H. Chemical and mineralogical compositions of silicic, mafic, and alkali tonsteins in the late Permian coals from the Songzao Coalfield, Chongqing, Southwest China. *Chem. Geol.* **2011**, *282*, 29–44. [[CrossRef](#)]
81. Liu, H.J. *Sedimentary Facies and Paleogeographic Study of Junger Coalfield*; Geology Press: Beijing, China, 1991.
82. Wang, Q.; Dai, S.; Nechaev, V.P.; French, D.; Graham, I.; Zhao, L.; Zhang, S.; Liang, Y.; Hower, J.C. Transformation of organic to inorganic nitrogen in NH<sub>4</sub><sup>+</sup>-illite-bearing and Ga-Al-REE-rich bituminous coals: Evidence from nitrogen isotopes and functionalities. *Chem. Geol.* **2024**, *660*, 122169. [[CrossRef](#)]
83. Zhao, L.; Dai, S.F.; Nechaev, V.P.; Nechaeva, E.V.; Graham, I.T.; French, D.; Sun, J.H. Enrichment of critical elements (Nb-Ta-Zr-Hf-REE) within coal and host rocks from the Datanhao mine, Daqingshan Coalfield, northern China. *Ore Geol. Rev.* **2019**, *111*, 102951. [[CrossRef](#)]
84. Zhao, L.; Sun, J.H.; Guo, W.M.; Wang, P.P.; Ji, D.P. Mineralogy of the Pennsylvanian coal seam in the Datanhao mine, Daqingshan Coalfield, Inner Mongolia, China: Genetic implications for mineral matter in coal deposited in an intermontane basin. *Int. J. Coal Geol.* **2016**, *167*, 201–214. [[CrossRef](#)]
85. Wang, S.L.; Ge, L.M. Geochemical Characteristics of Rare Earth Elements in Kaolin Rock from Daqingshan Coalfield. *Coal Geol. Explor.* **2007**, *35*, 5, (In Chinese with English Abstract).
86. Zhang, H.; Jia, B.W. Microscopic characters of kaolinite from the dirt band in a mega-thick coal seam, daqingshan and their genetic significance. *Acta Mineral. Sin.* **2000**, *20*, 117–120.
87. Zhong, R.; Sun, S.P.; Chen, F.; Fu, Z.M. The Discovery of Rhyo-tuffite in the Taiyuan Formation and Stratigraphic Correlation of the Daqingshan and Datong Coalfields. *Acta Geosci. Sin.* **1995**, *16*, 291–301.
88. Zhou, A.C.; Jia, B.W. Analysis of Late Paleozoic Conglomerates from Daqing Mountain in Inner Mongolia. *J. Taiyuan Univ. Technol.* **2000**, *31*, 498–504, (In Chinese with English abstract).
89. Jia, B.W.; Wu, Y.Q. The Provenance and Stratigraphic Significance of Volcanic Event Layers in Late Paleozoic Coal Measures from Daqingshan, Inner Mongolia. *J. Coal Mine Res. North. China* **1995**, *10*, 203–213.
90. Zhong, R.; Chen, F. *Coal-Bearing Construction in the Daqingshan Coalfield*; Geological Press: Beijing, China, 1988; p. 64, (In Chinese with English Abstract).
91. Hower, J.C.; Granite, E.J.; Mayfield, D.B.; Lewis, A.S.; Finkelman, R.B. Notes on Contributions to the Science of Rare Earth Element Enrichment in Coal and Coal Combustion Byproducts. *Minerals* **2016**, *6*, 32. [[CrossRef](#)]
92. Dai, S.F.; Zhao, L.; Peng, S.P.; Chou, C.L.; Wang, X.B.; Zhang, Y.; Li, D.; Sun, Y.Y. Abundances and distribution of minerals and elements in high-alumina coal fly ash from the Jungar Power Plant, Inner Mongolia, China. *Int. J. Coal Geol.* **2010**, *81*, 320–332. [[CrossRef](#)]
93. Kolker, A.; Scott, C.; Hower, J.C.; Vazquez, J.A.; Lopano, C.L.; Dai, S. Distribution of rare earth elements in coal combustion fly ash, determined by SHRIMP-RG ion microprobe. *Int. J. Coal Geol.* **2017**, *184*, 1–10. [[CrossRef](#)]
94. Liu, J.; Dai, S.; He, X.; Hower, J.C.; Sakulpitakphon, T. Size-Dependent Variations in Fly Ash Trace Element Chemistry: Examples from a Kentucky Power Plant and with Emphasis on Rare Earth Elements. *Energy Fuels* **2017**, *31*, 438–447. [[CrossRef](#)]
95. Dai, S.F.; Li, T.J.; Jiang, Y.F.; Ward, C.R.; Hower, J.C.; Sun, J.H.; Liu, J.J.; Song, H.J.; Wei, J.P.; Li, Q.Q.; et al. Mineralogical and geochemical compositions of the Pennsylvanian coal in the Hailiushu Mine, Daqingshan Coalfield, Inner Mongolia, China: Implications of sediment-source region and acid hydrothermal solutions. *Int. J. Coal Geol.* **2015**, *137*, 92–110. [[CrossRef](#)]
96. Wang, Q.; Dai, S.F.; French, D.; Spiro, B.; Graham, I.; Liu, J.J. Hydrothermally-altered coal from the Daqingshan Coalfield, Inner Mongolia, northern China: Evidence from stable isotopes of C within organic matter and C-O-Sr in associated carbonates. *Int. J. Coal Geol.* **2023**, *276*, 104330. [[CrossRef](#)]
97. Dai, S.F.; Zou, J.H.; Jiang, Y.F.; Ward, C.R.; Wang, X.B.; Li, T.; Xue, W.F.; Liu, S.D.; Tian, H.M.; Sun, X.H.; et al. Mineralogical and geochemical compositions of the Pennsylvanian coal in the Adaohai Mine, Daqingshan Coalfield, Inner Mongolia, China: Modes of occurrence and origin of diasporite, gorceixite, and ammonian illite. *Int. J. Coal Geol.* **2012**, *94*, 250–270. [[CrossRef](#)]

98. Li, J.; Wang, J.W.; Zhang, H.; Feng, X.D.; Yuan, W.; Zhang, X.Y.; Wang, Y.; Guo, S.; Cai, H.G.; Li, W.H. The co-enrichment mechanism and resource potential of Al-Ga-Li-Nb(Ta)- Zr(Hf) in Laosangou coal exploration area, Jungar coalfield. *Acta Geol. Sin.* **2024**, *98*, 2299–2315.
99. Seredin, V.V. A New Method for Primary Evaluation of the Outlook for Rare Earth Element Ores. *Geol. Ore Depos.* **2010**, *52*, 428–433. [[CrossRef](#)]
100. Chatterjee, S.; Mastalerz, M.; Drobniak, A.; Karacan, C.Ö. Machine learning and data augmentation approach for identification of rare earth element potential in Indiana Coals, USA. *Int. J. Coal Geol.* **2022**, *259*, 104054. [[CrossRef](#)]
101. Di, S.B.; Dai, S.F.; Nechaev, V.P.; Zhang, S.W.; French, D.; Graham, I.T.; Spiro, B.; Finkelman, R.B.; Hou, Y.J.; Wang, Y.C.; et al. Granite-bauxite provenance of abnormally enriched boehmite and critical elements (Nb, Ta, Zr, Hf and Ga) in coals from the Eastern Surface Mine, Ningwu Coalfield, Shanxi Province, China. *J. Geochem. Explor.* **2022**, *239*, 107016. [[CrossRef](#)]
102. Harrar, H.; Eterigho-Ikelegbe, O.; Modiga, A.; Bada, S. Mineralogy and distribution of rare earth elements in the Waterberg coalfield high ash coals. *Miner. Eng.* **2022**, *183*, 107611. [[CrossRef](#)]
103. Hower, J.C.; Eble, C.F.; Hopps, S.D.; Morgan, T.D. Aspects of rare earth element geochemistry of the Pond Creek coalbed, Pike County, Kentucky. *Int. J. Coal Geol.* **2022**, *261*, 104082. [[CrossRef](#)]
104. Moore, T.A.; Dai, S.F.; Huguet, C.; Pearse, J.; Liu, J.J.; Esterle, J.S.; Jia, R.K. Petrographic and geochemical characteristics of selected coal seams from the Late Cretaceous-Paleocene Guaduas Formation, Eastern Cordillera Basin, Colombia. *Int. J. Coal Geol.* **2022**, *259*, 104042. [[CrossRef](#)]
105. Wang, N.; Dai, S.F.; Wang, X.B.; Nechaev, V.P.; French, D.; Graham, I.T.; Zhao, L.; Song, X.L. New insights into the origin of Middle to Late Permian volcanoclastics (Nb-Zr-REY-Ga-rich horizons) from eastern Yunnan, SW China. *Lithos* **2022**, *420*, 106702. [[CrossRef](#)]
106. Zhang, J.; Falandysz, J.; Hanc, A.; Lorenc, W.; Wang, Y.Z.; Baralkiewicz, D. Occurrence, distribution, and associations of essential and non-essential elements in the medicinal and edible fungus “Fuling” from southern China. *Sci. Total Environ.* **2022**, *831*, 155011. [[CrossRef](#)] [[PubMed](#)]
107. Zhao, L.; Wang, X.; Dai, S. Lithium resources in coal-bearing strata: Occurrence, mineralization, and resource potential. *J. Coal Soc.* **2022**, *47*, 1750–1760, (In Chinese with English Abstract).
108. Shao, P.; Hou, H.J.; Wang, W.L.; Qin, K.M.; Wang, W.F. Distribution and enrichment of Al-Li-Ga-REEs in the High-Alumina coal of the Datong Coalfield, Shanxi Province, China. *Ore Geol. Rev.* **2022**, *140*, 104597. [[CrossRef](#)]
109. Talan, D.; Huang, Q.Q. A review study of rare Earth, Cobalt, Lithium, and Manganese in Coal-based sources and process development for their recovery. *Miner. Eng.* **2022**, *189*, 107897. [[CrossRef](#)]
110. Wang, X.M.; Wang, X.M.; Pan, Z.J.; Pan, W.H.; Yin, X.B.; Chai, P.C.; Pan, S.D.; Yang, Q. Mineralogical and geochemical characteristics of the Permian coal from the Qinshui Basin, northern China, with emphasis on lithium enrichment. *Int. J. Coal Geol.* **2019**, *214*, 103254. [[CrossRef](#)]
111. Zhao, L.; Dai, S.F.; Nechaev, V.P.; Nechaeva, E.V.; Graham, I.T.; French, D. Enrichment origin of critical elements (Li and rare earth elements) and a Mo-U-Se-Re assemblage in Pennsylvanian anthracite from the Jincheng Coalfield, southeastern Qinshui Basin, northern China. *Ore Geol. Rev.* **2019**, *115*, 103184. [[CrossRef](#)]
112. Zhou, M.X.; Zhao, L.; Wang, X.B.; Nechaev, V.P.; French, D.; Spiro, B.F.; Graham, I.T.; Hower, J.C.; Dai, S.F. Mineralogy and geochemistry of the Late Triassic coal from the Caotang mine, northeastern Sichuan Basin, China, with emphasis on the enrichment of the critical element lithium. *Ore Geol. Rev.* **2021**, *139*, 104582. [[CrossRef](#)]
113. Liu, J.; Dai, S.; Song, H.; Nechaev, V.P.; French, D.; Spiro, B.F.; Graham, I.T.; Hower, J.C.; Shao, L.; Zhao, J. Geological factors controlling variations in the mineralogical and elemental compositions of Late Permian coals from the Zhijin-Nayong Coalfield, western Guizhou, China. *Int. J. Coal Geol.* **2021**, *247*, 103855. [[CrossRef](#)]
114. Spiro, B.F.; Liu, J.; Dai, S.; Zeng, R.; Large, D.; French, D. Marine derived <sup>87</sup>Sr/<sup>86</sup>Sr in coal, a new key to geochronology and palaeoenvironment: Elucidation of the India-Eurasia and China-Indochina collisions in Yunnan, China. *Int. J. Coal Geol.* **2019**, *215*, 103304. [[CrossRef](#)]
115. Dai, S.; Ji, D.; Ward, C.R.; French, D.; Hower, J.C.; Yan, X.; Wei, Q. Mississippian anthracites in Guangxi Province, southern China: Petrological, mineralogical, and rare earth element evidence for high-temperature solutions. *Int. J. Coal Geol.* **2018**, *197*, 84–114. [[CrossRef](#)]
116. Ketris, M.P.; Yudovich, Y.E. Estimations of Clarkes for Carbonaceous biolithes: World averages for trace element contents in black shales and coals. *Int. J. Coal Geol.* **2009**, *78*, 135–148. [[CrossRef](#)]
117. Dai, S.F.; Ren, D.Y.; Li, S.S.; Zhao, L.; Zhang, Y. Coal facies evolution of the main minable coal-bed in the Heidaigou Mine, Jungar Coalfield, Inner Mongolia, northern China. *Sci. China Ser. D-Earth Sci.* **2007**, *50*, 144–152. [[CrossRef](#)]
118. Jiu, B.; Jin, Z.J.; Wang, Z.G.; Liu, R.C.; Hu, Q.T. Modes of occurrence of gallium in Al-Ga-rich coals in the Jungar Coalfield, Ordos Basin, China: Insights from LA-ICP-MS data. *Int. J. Coal Geol.* **2024**, *282*, 104436. [[CrossRef](#)]

119. Li, J.; Zhuang, X.G.; Yuan, W.; Liu, B.; Querol, X.; Font, O.; Moreno, N.; Li, J.F.; Gang, T.; Liang, G.K. Mineral composition and geochemical characteristics of the Li-Ga-rich coals in the Buertaohai-Tianjiashipan mining district, Jungar Coalfield, Inner Mongolia. *Int. J. Coal Geol.* **2016**, *167*, 157–175. [[CrossRef](#)]
120. Wang, X.B.; Dai, S.F.; Sun, Y.Y.; Li, D.; Zhang, W.G.; Zhang, Y.; Luo, Y.B. Modes of occurrence of fluorine in the Late Paleozoic No. 6 coal from the Haerwusu Surface Mine, Inner Mongolia, China. *Fuel* **2011**, *90*, 248–254. [[CrossRef](#)]
121. *ASTM Standard D388-12*; Classification of Coals by Rank. ASTM International: West Conshohocken, PA, USA, 2012.
122. Dai, S.F.; Hou, X.Q.; Ren, D.Y.; Tang, Y.G. Surface analysis of pyrite in the No. 9 coal seam, Wuda Coalfield, Inner Mongolia, China, using high-resolution time-of-flight secondary ion mass-spectrometry. *Int. J. Coal Geol.* **2003**, *55*, 139–150. [[CrossRef](#)]
123. Dai, S.F.; Ren, D.Y.; Tang, Y.G.; Shao, L.Y.; Li, S.S. Distribution, isotopic variation and origin of sulfur in coals in the Wuda coalfield, Inner Mongolia, China. *Int. J. Coal Geol.* **2002**, *51*, 237–250. [[CrossRef](#)]
124. Liu, J.; Ward, C.R.; Graham, I.T.; French, D.; Dai, S.; Song, X. Modes of occurrence of non-mineral inorganic elements in lignites from the Mile Basin, Yunnan Province, China. *Fuel* **2018**, *222*, 146–155. [[CrossRef](#)]
125. Liu, J.; Yang, Z.; Yan, X.; Ji, D.; Yang, Y.; Hu, L. Modes of occurrence of highly-elevated trace elements in superhigh-organic-sulfur coals. *Fuel* **2015**, *156*, 190–197. [[CrossRef](#)]
126. Johnston, M.N.; Hower, J.C.; Dai, S.F.; Wang, P.P.; Xie, P.P.; Liu, J.J. Petrology and Geochemistry of the Harlan, Kellioka, and Darby Coals from the Louellen 7.5-Minute Quadrangle, Harlan County, Kentucky. *Minerals* **2015**, *5*, 894–918. [[CrossRef](#)]
127. Finkelman, R.B. Trace and minor elements in coal. In *Organic Geochemistry*; Engel, M.H., Macko, S., Eds.; Plenum: New York, NY, USA, 1993; pp. 593–607.
128. Palmer, C.A.; Tuncali, E.; Dennen, K.O.; Coburn, T.C.; Finkelman, R.B. Characterization of Turkish coals: A nationwide perspective. *Int. J. Coal Geol.* **2004**, *60*, 85–115. [[CrossRef](#)]
129. Dai, S.F.; Chou, C.L.; Yue, M.; Luo, K.L.; Ren, D.Y. Mineralogy and geochemistry of a Late Permian coal in the Dafang Coalfield, Guizhou, China: Influence from siliceous and iron-rich calcic hydrothermal fluids. *Int. J. Coal Geol.* **2005**, *61*, 241–258. [[CrossRef](#)]
130. Finkelman, R.B.; Palmer, C.A.; Wang, P. Quantification of the modes of occurrence of 42 elements in coal. *Int. J. Coal Geol.* **2018**, *185*, 138–160. [[CrossRef](#)]
131. Finkelman, R.B. Potential health impacts of burning coal beds and waste banks. *Int. J. Coal Geol.* **2004**, *59*, 19–24. [[CrossRef](#)]
132. Finkelman, R.B.; Orem, W.; Castranova, V.; Tatu, C.A.; Belkin, H.E.; Zheng, B.S.; Lerch, H.E.; Maharaj, S.V.; Bates, A.L. Health impacts of coal and coal use: Possible solutions. *Int. J. Coal Geol.* **2002**, *50*, 425–443. [[CrossRef](#)]
133. Davis, B.A.; Rodrigues, S.; Esterle, J.S.; Nguyen, A.D.; Duxbury, A.J.; Golding, S.D. Geochemistry of apatite in Late Permian coals, Bowen Basin, Australia. *Int. J. Coal Geol.* **2021**, *237*, 103708. [[CrossRef](#)]
134. Hower, J.C.; Campbell, J.L.; Teesdale, W.J.; Nejedly, Z.; Robertson, J.D. Scanning proton microprobe analysis of mercury and other trace elements in Fe-sulfides from a Kentucky coal. *Int. J. Coal Geol.* **2008**, *75*, 88–92. [[CrossRef](#)]
135. Kolker, A. Minor element distribution in iron disulfides in coal: A geochemical review. *Int. J. Coal Geol.* **2012**, *94*, 32–43. [[CrossRef](#)]
136. Matysek, D.; Jirásek, J. Mineralogy of the coal waste dumps from the Czech part of the Upper Silesian Basin: Emphasized role of halides for element mobility. *Int. J. Coal Geol.* **2022**, *264*, 104138. [[CrossRef](#)]
137. Dai, S.F.; Luo, Y.B.; Seregin, V.V.; Ward, C.R.; Hower, J.C.; Zhao, L.; Liu, S.D.; Zhao, C.L.; Tian, H.M.; Zou, J.H. Revisiting the late Permian coal from the Huayingshan, Sichuan, southwestern China: Enrichment and occurrence modes of minerals and trace elements. *Int. J. Coal Geol.* **2014**, *122*, 110–128. [[CrossRef](#)]
138. Dai, S.F.; Zhou, Y.P.; Zhang, M.Q.; Wang, X.B.; Wang, J.M.; Song, X.L.; Jiang, Y.F.; Luo, Y.B.; Song, Z.T.; Yang, Z.; et al. A new type of Nb (Ta)-Zr(Hf)-REE-Ga polymetallic deposit in the late Permian coal-bearing strata, eastern Yunnan, southwestern China: Possible economic significance and genetic implications. *Int. J. Coal Geol.* **2010**, *83*, 55–63. [[CrossRef](#)]
139. Wang, N.; Dai, S.; Nechaev, V.P.; French, D.; Graham, I.T.; Song, X.; Chekryzhov, I.Y.; Tarasenko, I.A.; Budnitskiy, S.Y. Detrital UPb zircon geochronology, zircon LuHf and SrNd isotopic signatures of the Lopingian volcanic-ash-derived Nb-Zr-REY-Ga mineralized horizons from eastern Yunnan, SW China. *Lithos* **2024**, *468–469*, 107494. [[CrossRef](#)]
140. Wang, N.; French, D.; Dai, S.; Graham, I.T.; Zhao, L.; Song, X.; Zheng, J.; Gao, Y.; Wang, Y. Origin of chamosite and berthierine: Implications for volcanic-ash-derived Nb-Zr-REY-Ga mineralization in the Lopingian sequences from eastern Yunnan, SW China. *J. Asian Earth Sci.* **2023**, *253*, 105703. [[CrossRef](#)]
141. Wang, N.; Dai, S.; Nechaev, V.P.; French, D.; Graham, I.T.; Zhao, F.; Zuo, J. Isotopes of carbon and oxygen of siderite and their genetic indications for the Late Permian critical-metal tuffaceous deposits (Nb-Zr-REY-Ga) from Yunnan, southwestern China. *Chem. Geol.* **2022**, *592*, 120727. [[CrossRef](#)]
142. Dai, S.; Nechaev, V.P.; Chekryzhov, I.Y.; Zhao, L.; Vysotskiy, S.V.; Graham, I.; Ward, C.R.; Ignatiev, A.V.; Velivetskaya, T.A.; Zhao, L.; et al. A model for Nb–Zr–REE–Ga enrichment in Lopingian altered alkaline volcanic ashes: Key evidence of H–O isotopes. *Lithos* **2018**, *302–303*, 359–369. [[CrossRef](#)]
143. Zhao, L.; Dai, S.; Graham, I.T.; Li, X.; Liu, H.; Song, X.; Hower, J.C.; Zhou, Y. Cryptic sediment-hosted critical element mineralization from eastern Yunnan Province, southwestern China: Mineralogy, geochemistry, relationship to Emeishan alkaline magmatism and possible origin. *Ore Geol. Rev.* **2017**, *80*, 116–140. [[CrossRef](#)]

144. Zhao, L.X.; Dai, S.F.; Graham, I.T.; Wang, P.P. Clay Mineralogy of Coal-Hosted Nb-Zr-REE-Ga Mineralized Beds from Late Permian Strata, Eastern Yunnan, SW China: Implications for Paleotemperature and Origin of the Micro-Quartz. *Minerals* **2016**, *6*, 45. [[CrossRef](#)]
145. Zhao, L.; Dai, S.; Graham, I.T.; Li, X.; Zhang, B. New insights into the lowest Xuanwei Formation in eastern Yunnan Province, SW China: Implications for Emeishan large igneous province felsic tuff deposition and the cause of the end-Guadalupian mass extinction. *Lithos* **2016**, *264*, 375–391. [[CrossRef](#)]
146. Anggara, F.; Patria, A.A.; Rahmat, B.; Wibisono, H.; Putera, M.Z.J.; Petrus, H.T.B.M.; Erviana, F.; Handini, E.; Amijaya, D.H. Signature characteristics of coal geochemistry from the Eocene Tanjung Formation and the Miocene Warukin Formation, Barito Basin: Insights into geological control on coal deposition and future critical element prospecting. *Int. J. Coal Geol.* **2024**, *282*, 104423. [[CrossRef](#)]
147. Karayığit, A.İ.; Oskay, R.G.; Córdoba Sola, P.; Bulut, Y.; Eminağaoğlu, M. Mineralogical and elemental composition of the Middle Miocene coal seams from the Alpu coalfield (Eskişehir, Central Türkiye): Insights from syngenetic zeolite formation. *Int. J. Coal Geol.* **2024**, *282*, 104408. [[CrossRef](#)]
148. Pearce, J.K.; Blach, T.; Dawson, G.K.W.; Southam, G.; Paterson, D.J.; Golding, S.D.; Bahadur, J.; Melnichenko, Y.B.; Rudolph, V. Cooper Basin REM gas shales after CO<sub>2</sub> storage or acid reactions: Metal mobilisation and methane accessible pore changes. *Int. J. Coal Geol.* **2023**, *273*, 104271. [[CrossRef](#)]
149. Shen, M.L.; Dai, S.F.; French, D.; Graham, I.T.; Spiro, B.F.; Wang, N.; Tian, X. Geochemical and mineralogical evidence for the formation of siderite in Late Permian coal-bearing strata from western Guizhou, SW China. *Chem. Geol.* **2023**, *637*, 121675. [[CrossRef](#)]
150. Tuncer, A.; Karayığit, A.I.; Oskay, R.G.; Tunoğlu, C.; Kayseri-Özer, M.S.; Gümüş, B.A.; Bulut, Y.; Akbulut, A. A multi-proxy record of palaeoenvironmental and palaeoclimatic conditions during Plio-Pleistocene peat accumulation in the eastern flank of the Isparta Angle: A case study from the Şarkikaraağaç coalfield (Isparta, SW Central Anatolia). *Int. J. Coal Geol.* **2023**, *265*, 104149. [[CrossRef](#)]
151. Dai, S.; Chou, C.L. Occurrence and origin of minerals in a chamosite-bearing coal of Late Permian age, Zhaotong, Yunnan, China. *Am. Miner.* **2007**, *92*, 1253–1261. [[CrossRef](#)]
152. Dai, S.F.; Tian, L.W.; Chou, C.L.; Zhou, Y.P.; Zhang, M.Q.; Zhao, L.; Wang, J.M.; Yang, Z.; Cao, H.Z.; Ren, D.Y. Mineralogical and compositional characteristics of Late Permian coals from an area of high lung cancer rate in Xuan Wei, Yunnan, China: Occurrence and origin of quartz and chamosite. *Int. J. Coal Geol.* **2008**, *76*, 318–327. [[CrossRef](#)]
153. Suchy, V.; Zacharias, J.; Sykorova, I.; Korinkova, D.; Pesek, J.; Brabcova, K.P.; Luo, Q.Y.; Filip, J.; Svetlik, I. Palaeo-thermal history of the Blanice Graben (the Bohemian Massif, Czech Republic): The origin of anthracite in a late-Variscan strike-slip basin. *Int. J. Coal Geol.* **2022**, *263*, 104129. [[CrossRef](#)]
154. Dai, S.F.; Ren, D.Y. Effects of magmatic intrusion on mineralogy and geochemistry of coals from the Fengfeng-Handan coalfield, Hebei, China. *Energy Fuels* **2007**, *21*, 1663–1673. [[CrossRef](#)]
155. Finkelman, R.B.; Bostick, N.H.; Dulong, F.T.; Senftle, F.E.; Thorpe, A.N. Influence of an igneous intrusion on the inorganic geochemistry of a bituminous coal from Pitkin County, Colorado. *Int. J. Coal Geol.* **1998**, *36*, 223–241. [[CrossRef](#)]
156. Sanders, M.M.; Rimmer, S.M. Revisiting the thermally metamorphosed coals of the Transantarctic Mountains, Antarctica. *Int. J. Coal Geol.* **2020**, *228*, 103550. [[CrossRef](#)]
157. Rimmer, S.M.; Yoksoulian, L.E.; Hower, J.C. Anatomy of an intruded coal, I: Effect of contact metamorphism on whole-coal geochemistry, Springfield (No. 5) (Pennsylvanian) coal, Illinois Basin. *Int. J. Coal Geol.* **2009**, *79*, 74–82. [[CrossRef](#)]
158. Dai, S.F.; Hower, J.C.; Ward, C.R.; Guo, W.M.; Song, H.J.; O’Keefe, J.M.K.; Xie, P.P.; Hood, M.M.; Yan, X.Y. Elements and phosphorus minerals in the middle Jurassic inertinite-rich coals of the Muli Coalfield on the Tibetan Plateau. *Int. J. Coal Geol.* **2015**, *144*, 23–47. [[CrossRef](#)]
159. Hower, J.C.; Groppo, J.G.; Eble, C.F.; Hopps, S.D.; Morgan, T.D. Was coal metamorphism an influence on the minor element chemistry of the Middle Pennsylvanian Springfield (No. 9) coal in Western Kentucky? *Int. J. Coal Geol.* **2023**, *274*, 104295. [[CrossRef](#)]
160. Hower, J.C.; Gebremedhin, M.; Zourarakis, D.P.; Finkelman, R.B.; French, D.; Graham, I.T.; Schobert, H.H.; Zhao, L.; Dai, S. Is Hyperaccumulation A Viable Hypothesis for Organic Associations of Minor Elements in Coals? *Earth-Sci. Rev.* **2024**, *254*, 104802. [[CrossRef](#)]
161. Xie, P.P.; Dai, S.F.; Hower, J.C.; Nechaev, V.P.; French, D.; Graham, I.T.; Wang, X.B.; Zhao, L.; Zuo, J.P. Nitrogen isotopic compositions in NH<sub>4</sub><sup>+</sup>-mineral-bearing coal: Origin and isotope fractionation. *Chem. Geol.* **2021**, *559*, 119946. [[CrossRef](#)]
162. Han, Q.; Liu, J.; Hower, J.C.; Moore, T.A.; Shang, N.; Zhao, S.; Jia, R.; Dai, S. Fire activities and their impacts on local ecosystems in the southern Ordos Basin during the Middle Jurassic: Evidence from pyrogenic PAHs and petrography of inertinite-rich coal. *Palaeogeogr. Palaeoclimatol. Palaeoecol.* **2024**, *636*, 111972. [[CrossRef](#)]

163. Liu, J.; Dai, S.; Hower, J.C.; Moore, T.A.; Moroeng, O.M.; Nechaev, V.P.; Petrenko, T.I.; French, D.; Graham, I.T.; Song, X. Stable isotopes of organic carbon, palynology, and petrography of a thick low-rank Miocene coal within the Mile Basin, Yunnan Province, China: Implications for palaeoclimate and sedimentary conditions. *Org. Geochem.* **2020**, *149*, 104103. [[CrossRef](#)]
164. Sanders, M.M.; Rimmer, S.M.; Rowe, H.D. Carbon isotopic composition and organic petrography of thermally metamorphosed Antarctic coal: Implications for evaluation of  $\delta^{13}\text{C}_{\text{org}}$  excursions in paleo-atmospheric reconstruction. *Int. J. Coal Geol.* **2023**, *267*, 104182. [[CrossRef](#)]
165. Bał, K.; Szram, E.; Zielińska, M.; Misz-Kennan, M.; Fabiańska, M.; Bał, M.; Górny, Z. Organic matter variations in the deep marginal basin of the Western Tethys and links to various environments in isotopic Albian–Cenomanian Boundary Interval. *Int. J. Coal Geol.* **2023**, *266*, 104181. [[CrossRef](#)]
166. Zhou, M.X.; Dai, S.F.; Wang, Z.; Spiro, B.F.; Vengosh, A.; French, D.; Graham, I.T.; Zhao, F.H.; Zuo, J.P.; Zhao, J.T. The Sr isotope signature of Wuchiapingian semi-anthracites from Chongqing, southwestern China: Indication for hydrothermal effects. *Gondwana Res.* **2022**, *103*, 522–541. [[CrossRef](#)]
167. Mills, S. *Rare Earth Elements—Recovery from Coal Based Materials*; ICSC/334; International Centre for Sustainable Carbon: London, UK, 2024; p. 96.
168. Zhao, L.; Dai, S.; Finkelman, R.B.; French, D.; Graham, I.T.; Yang, Y.; Li, J.; Yang, P. Leaching behavior of trace elements from fly ashes of five Chinese coal power plants. *Int. J. Coal Geol.* **2020**, *219*, 103381. [[CrossRef](#)]
169. Zhang, S.; Dai, S.; Finkelman, R.B.; Graham, I.T.; French, D.; Hower, J.C.; Li, X. Leaching characteristics of alkaline coal combustion by-products: A case study from a coal-fired power plant, Hebei Province, China. *Fuel* **2019**, *255*, 115710. [[CrossRef](#)]
170. Dai, S.; Finkelman, R.B. Coal geology in China: An overview. *Int. Geol. Rev.* **2018**, *60*, 531–534. [[CrossRef](#)]

**Disclaimer/Publisher’s Note:** The statements, opinions and data contained in all publications are solely those of the individual author(s) and contributor(s) and not of MDPI and/or the editor(s). MDPI and/or the editor(s) disclaim responsibility for any injury to people or property resulting from any ideas, methods, instructions or products referred to in the content.